sition and placed in the beam of the Nicolet R3m diffractometer. Unit-cell dimensions were obtained from a least-squares fit to the setting angles for 25 reflections (2θ(av) = 17.88°). Details of the crystallographic experiment and computations for 5 are listed in Table I. All data processing was performed on a DG Eclipse/S140 computer using the SHELXTL program library, version 5.1.[40] An empirical absorption correction was performed by using the azimuthal data from 13 ψ-scan reflections collected in 12° increments; maximum transmission factor was 0.030, minimum transmission factor was 0.015. Neutral atom scattering factors and anomalous scattering contributions[41] were used for all non-hydrogen atoms.

Analysis of the Patterson map established the positions of the iron and tungsten atoms. Subsequent ΔF electron density maps revealed all non-hydrogen atoms. All non-hydrogen atoms were refined with anisotropic thermal parameters.

Hydrogen atoms placed in idealized positions (C–H = 0.96 Å, $U_H = 1.2U_{iso}$, C). In the final ΔF map, the highest peak (1.16 e Å^{-3}) was located 0.85 Å from tungsten. Final fractional atomic coordinates and thermal parameters with esd's are listed in Tables S-1–5. A table of calculated vs observed structure factors is available as supplementary material, Table S-6.

X-ray Data Collection and Structure Determination for 8. Crystals of $CH_3(CO)_3W(\eta^5\text{-}C_5H_4PPh_2)FeCp(CO)(COCH_3)$ (8) suitable for X-ray diffraction measurements were obtained by layering pentane on a dichloromethane solution of 8 and cooling for 5 days at −20 °C. The orange, clear crystal chosen for the experiment was coated with epoxy in order to retard decomposition. Unit-cell dimensions were obtained from a least-squares fit to the setting angles for 25 reflections (2θ(av) = 24.04°). Details of the crystallographic experiment and computations for 8 are listed in Table III. An empirical absorption correction was performed by using the azimuthal data from 15 ψ-scan reflections collected in 15° increments, maximum transmission factor was 0.768, minimum transmission factor was 0.522.

Analysis of the Patterson map established the positions of the iron and tungsten atoms. Subsequent ΔF electron density maps revealed all non-hydrogen atoms. All non-hydrogen atoms were refined with anisotropic thermal parameters.

Hydrogen atoms were placed in idealized positions. In the final ΔF map, the highest peak (1.3 e Å^{-3}), was located 0.87 Å from tungsten. Final fractional atomic coordinates and thermal parameters with esd's are listed in Tables S-7–11. A table of calculated vs observed structure factors is available as supplementary material (Table S-12).

Acknowledgment. This research was supported by the Department of Energy, Contract DE-FG02-85ER13340. The Nicolet R3m/E X-ray diffractometer and computing system at Colorado State University was purchased with funds provided by the National Science Foundation.

Registry No. 1, 12080-06-7; 2, 12082-27-8; 3, 119455-51-5; 4, 119455-52-6; 5, 119455-53-7; 6, 119455-54-8; 7, 119455-56-0; 8, 119455-57-1; 10, 119455-58-2; 12, 119455-59-3; $W(CO)_6$, 14040-11-0; CpNa, 4984-82-1; $CpW(CO)_3Cl$, 12128-24-4; $CpW(CO)_3H$, 12128-26-6.

Supplementary Material Available: Table S-1, atomic coordinates ($\times 10^4$) and isotropic thermal parameters (Å$^2 \times 10^3$)[a] for 5, Table S-2, bond lengths (Å) for 5, Table S-3, bond angles (deg) for 5, Table S-4, anisotropic thermal parameters (Å$^2 \times 10^3$) for 5, Table S-5, hydrogen coordinates ($\times 10^4$) and thermal parameters (Å$^2 \times 10^3$) for 5, Table S-7, atomic coordinates ($\times 10^4$) and isotropic thermal parameters (Å$^2 \times 10^3$) for 8, Table S-8, bond lengths (Å) for 8, Table S-9, bond angles (deg) for 8, Table S-10, anisotropic thermal parameters (Å$^2 \times 10^3$) for 8, and Table S-11, hydrogen coordinates ($\times 10^4$) and thermal parameters (Å$^2 \times 10^3$) for 8 (13 pages); Table S-6, observed and calculated structure factors for 5, and Table S-12, observed and calculated structure factors for 8 (45 pages). Ordering information is given on any current masthead page.

(40) Sheldrick, G. M. SHELXTL, revision 5.1; Nicolet XRD Corp., Madison, WI, 1985.

(41) *International Tables for X-ray Crystallography*; Kynoch Press: Birmingham, England, 1974; Vol. IV, p 99.

Cluster-Bound Ylides Derived from CCO. Conversion of $[Fe_2Co(CO)_9(CCO)]^-$ to $[Fe_2Co(CO)_9(CPR_3)]^-$

Stanton Ching, Michal Sabat, and Duward F. Shriver*

Department of Chemistry, Northwestern University, Evanston, Illinois 60208

Received September 14, 1988

The ketenylidene-containing cluster $[PPN][Fe_2Co(CO)_9(CCO)]$ (1) reacts with a variety of simple phosphines to produce cluster-bound phosphorus ylides. The reactions proceed by a two-step process in which initial substitution at the Co metal center to give $[PPN][Fe_2Co(CO)_8(PR_3)(CCO)]$ (**2a–f**) is followed by phosphine migration to generate the organometallic ylides $[PPN][Fe_2Co(CO)_9(CPR_3)]$ (**3a–e**) (**a**, R = PMe_3; **b**, R = PMe_2Ph; **c**, R = $PMePh_2$; **d**, R = PEt_3; **e**, R = $P(OMe)_3$; **f**, R = $P(OPh)_3$). The substitution reaction does not occur for the bulky phosphines PPh_3 and PCy_3. The rate of the migration step appears sensitive to phosphine basicity. The compound $[PPN][Fe_2Co(CO)_9(CPMe_3)]$ (**3a**) undergoes protonation at the metal framework to give $HFe_2Co(CO)_9(CPMe_3)$, whereas the reaction with $Co_2(CO)_8$ generates a butterfly carbide cluster, $Fe_2Co_2(C)(CO)_{11}(PMe_3)$. Treatment of 1 with dmpm (dmpm = bis(dimethylphosphino)methane) produces $[PPN][Fe_2Co(CO)_7(dmpm)(CCO)]$ (6), which retains the ketenylidene moiety. This cluster undergoes CO exchange and electrophilic attack more readily than 1. The X-ray crystal structures of **3a** and $\mathbf{6}\cdot CH_2Cl_2$ have been determined. Crystal data for **3a**: space group $P2_1/c$, $a = 14.370$ (3) Å, $b = 18.761$ (2) Å, $c = 17.621$ (3) Å, $\beta = 94.21$ (2)°, $V = 4738$ (2) Å^3, $Z = 4$. Crystal data for $\mathbf{6}\cdot CH_2Cl_2$: space group $P\bar{1}$, $a = 16.398$ (2) Å, $b = 16.858$ (2) Å, $c = 9.478$ (2) Å, $\alpha = 94.89$ (1)°, $\beta = 99.11$ (1)°, $\gamma = 93.06$ (1)°, $V = 2572$ (1) Å^3, $Z = 2$.

Introduction

Ketenylidene-containing clusters undergo a variety of ligand transformations upon treatment with nucleophiles and electrophiles.[1–7] In these processes, molecular charge plays a key role in determining how the cluster will react toward different substrates. We have previously described

(1) Geoffroy, G. L.; Bassner, S. L. *Adv. Organomet. Chem.* **1988**, *28*, 1.

(2) (a) Seyferth, D.; Hallgren, J. E.; Eschbach, C. S. *J. Am. Chem. Soc.* **1974**, *96*, 1730. (b) Seyferth, D.; Williams, G. H.; Nivert, C. L. *Inorg. Chem.* **1977**, *16*, 758.

(3) Ching, S.; Holt, E. M.; Kolis, J. W.; Shriver, D. F. *Organometallics* **1988**, *7*, 892.

0276-7333/89/2308-1047$01.50/0

how $[Fe_2Co(CO)_9(CCO)]^-$ is susceptible to nucleophilic attack in spite of its 1− charge.[3] By contrast, dinegatively charged ketenylidene clusters react with electrophiles.[4-7] The present research was motivated initially by our plan to use phosphine substitution for metal-bonded CO on $[Fe_2Co(CO)_9(CCO)]^-$ as a method of altering the reactivity of the cluster. However, the unexpected discovery that PMe_3 displaces CO from the capping carbon atom of $[Fe_2Co(CO)_9(CCO)]^-$ to afford the ylide-capped cluster $[Fe_2Co(CO)_9(CPMe_3)]^-$ (eq 1),[8] soon became the central

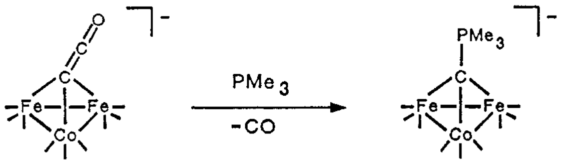

(1)

focus of the research. This unusual reaction demonstrates previously unobserved coordination chemistry for a carbide heteroatom of a metal cluster and represents the only instance of a formal nucleophilic attack at the capping carbon atom of a ketenylidene ligand.

The present report surveys the chemistry of phosphine derivatives of $[Fe_2Co(CO)_9(CCO)]^-$. Two series of phosphine-substituted derivatives, $[Fe_2Co(CO)_8(PR_3)(CCO)]^-$ and $[Fe_2Co(CO)_9(CPR_3)]^-$, have been generated and characterized in order to delineate factors that influence the conversion of a μ_3-CCO ligand into a cluster-bound ylide. The reactivity of $[Fe_2Co(CO)_9(CPMe_3)]^-$ has been examined to determine the stability of the ylide bonding. The synthesis, structure, and reactivity of $[Fe_2Co(CO)_7(dmpm)(CCO)]^-$ (dmpm = bis(dimethylphosphino)methane) are also presented. This cluster serves as an isolable model of the nonisolable $[Fe_2Co(CO)_8(PR_3)(CCO)]^-$ complexes.

Experimental Section

General Procedures and Materials. All manipulations were performed under a purified N_2 atmosphere by using standard Schlenk and syringe techniques[9] or in a Vacuum Atmospheres drybox, unless noted otherwise. Solvents were stored under N_2 after being refluxed with and distilled from appropriate drying agents: CH_2Cl_2, P_2O_5; Et_2O and THF, Na–benzophenone; acetone, hexane, and pentane, 4A molecular sieves; MeOH, Mg–I_2. Solvents for NMR spectroscopy were vacuum distilled from appropriate drying agents: CD_2Cl_2, P_2O_5; acetone-d_6 and $CHFCl_2$, 4A molecular sieves. PMe_3, PMe_2Ph, $PMePh_2$, PEt_3, $P(OMe)_3$, $P(OPh)_3$, and dmpm (bis(dimethylphosphino)methane) (Strem) were used as received. HSO_3CF_3 and $CH_3SO_3CF_3$ were distilled before use. MeI was stored in the dark over Cu mesh and vacuum distilled before use. $Co_2(CO)_8$ (Strem) was freshly sublimed before use. $[PPN][Fe_2Co(CO)_9(CCO)]$ was prepared by a published procedure[3] (PPN = bis(triphenylphosphine)nitrogen(1+)).

Column chromatography was carried out by using a 6-cm column (1.5 cm diameter) of Florisil (60–100 mesh, Aldrich) which was packed as a hexane slurry in air. A side arm at the top of the column allowed a continuous N_2 purge during elution. Solvents used for elution were reagent grade and were deaerated, but not dried, before use. Compounds eluted from the column were collected under N_2.

IR spectra were recorded with a Perkin-Elmer 283 spectrophotometer using CaF_2 solution cells with 0.1-mm path lengths. NMR spectra were recorded with either a JEOL FX-90Q (^{31}P, 36.19 MHz; ^{59}Co, 21.16 MHz), JEOL FX-270 (^{1}H, 269.65 MHz; ^{13}C, 67.80 MHz; ^{31}P, 109.16 MHz; ^{59}Co, 63.75 MHz), or Varian XL-400 (^{1}H, 399.942 MHz; ^{13}C, 100.577 MHz; ^{31}P, 161.905 MHz) spectrometer. NMR chemical shifts are reported with respect to standard references (^{1}H and ^{13}C, TMS; ^{31}P, 85% H_3PO_4; ^{59}Co, saturated, aqueous $K_3Co(CN)_6$), and deshielded resonances are taken as positive chemical shifts. ^{1}H and ^{13}C NMR shifts were referenced internally to residual solvent protons (^{1}H, $CHDCl_2$, 5.32 ppm) or solvent (^{13}C, CD_2Cl_2, 53.8 ppm). ^{31}P NMR shifts were referenced externally to an 85% H_3PO_4 standard, and ^{59}Co NMR shifts were referenced externally to a standard sample of saturated $K_3Co(CN)_6$ in D_2O. Mass spectra were recorded by Dr. D. L. Hung of the Northwestern University Analytical Services Laboratory with a Hewlett-Packard HP5905A spectrometer using 70-eV ionization. Elemental analyses were performed by Elbach Laboratories (FRG).

$[PPN][Fe_2Co(CO)_9(CPMe_3)]$ (3a). A 1.00-g (1.00-mmol) sample of $[PPN][Fe_2Co(CO)_9(CCO)]$ was dissolved in 12 mL of CH_2Cl_2 and treated with 0.12 mL (1.2 mmol) of PMe_3. After 30 min of stirring, the solution became red-brown and the solvent and excess PMe_3 was removed under vacuum. The resulting oil was dissolved in 20 mL of CH_2Cl_2 and filtered. The solution was concentrated to ca. 6 mL before 24 mL of Et_2O was added. Vigorous agitation first produced an oil and then red-orange crystals. After the solution was cooled to −78 °C for 4 h, the crystals were isolated by filtration, washed with Et_2O, and dried under vacuum. Yield: 0.86 g (82%). Anal. Calcd for $C_{49}H_{39}CoFe_2NO_9P_3$: C, 56.08; H, 3.72; P, 8.86; Fe, 10.65; Co, 5.62. Found: C, 55.96; H, 3.57; P, 9.04; Fe, 11.30; Co, 6.11.

$HFe_2Co(CO)_9(CPMe_3)$ (4). A 0.20-g (0.19-mmol) sample of $[PPN][Fe_2Co(CO)_9(CPMe_3)]$ was dissolved in 8 mL of CH_2Cl_2, and 20 μL (0.23 mmol) of HSO_3CF_3 was added with stirring. An immediate color change to orange-red was accompanied by the appearance of an insignificant amount of red solid (identified spectroscopically as $HFe_2Co(CO)_9(CPMe_3)$). After 5 min this solution was passed down a column of Florisil and eluted with CH_2Cl_2. A single orange-red band was collected. Subsequent removal of the solvent under vacuum left red crystals that were washed with hexane and vacuum dried. Yield: 0.06 g (62%). IR: (CH_2Cl_2) ν_{CO} 2074 (w), 2050 (m, sh), 2028 (vs), 2019 (vs), 1999 (s), 1972 (m, sh) cm^{-1}. MS: parent ion *m/e* 512 with successive loss of nine CO units. ^{1}H NMR (CD_2Cl_2, +25 °C): 2.02 (d, $^2J_{PH}$ = 12.2 Hz, $P(CH_3)_3$), −19.01 (s, HFe_2Co) ppm. ^{31}P NMR (CD_2Cl_2, −90 °C): 36.2 ppm. Anal. Calcd for $C_{13}H_{10}CoFe_2O_9P$: C, 30.51; H, 1.95. Found: C, 31.54; H, 1.92.

$Fe_2Co_2(C)(CO)_{11}(PMe_3)$ (5). A 0.40-g (0.38-mmol) sample of $[PPN][Fe_2Co(CO)_9(CPMe_3)]$ and 0.16 g (0.47 mmol) of $Co_2(CO)_8$ were dissolved in 8 mL of THF, and the mixture was stirred for 5 min. The solvent was removed under vacuum and the resulting oil dissolved in 6 mL of CH_2Cl_2. The solution was passed down a column of Florisil and eluted with CH_2Cl_2/hexane (1:1). A broad, red-purple band was collected, and the solvent was removed under vacuum, leaving purple-black crystals as a mixture of $Fe_2Co_2(C)(CO)_{11}(CPMe_3)$ and $Co_4(CO)_{12}$ (identified spectroscopically). The crystals were washed with three 5-mL portions of hexane to remove the $Co_4(CO)_{12}$ with some loss of $Fe_2Co_2(C)(CO)_{11}(PMe_3)$. The remaining crystals were vacuum dried. Yield: 0.06 g (25%). IR: (CH_2Cl_2) ν_{CO} 2084 (w), 2038 (s), 2023 (s, sh), 2000 (m), 1975 (w) cm^{-1}. MS: parent ion *m/e* 626 with successive loss of 11 CO units. ^{1}H NMR (CD_2Cl_2, +25 °C): 1.68 (d, $^2J_{PH}$ = 10.7 Hz) ppm. ^{31}P NMR (CD_2Cl_2, −90 °C) 18.0 ppm. Anal. Calcd for $C_{15}H_9Co_2Fe_2O_{11}P$: C, 28.79; H, 1.44; Fe, 17.85; Co, 18.84. Found: C, 29.09; H, 1.51; Fe, 17.20; Co, 17.85.

$[PPN][Fe_2Co(CO)_7(dmpm)(CCO)]\cdot CH_2Cl_2$ (6·CH_2Cl_2). A 2.00-g (2.00-mmol) sample of $[PPN][Fe_2Co(CO)_9(CCO)]$ was dissolved in 20 mL of CH_2Cl_2 and treated with 0.36 mL (2.4 mmol) of dmpm. After 4 h of stirring, the solution became red-brown and the solvent was removed under vacuum. The resulting oil was dissolved in 20 mL of CH_2Cl_2 and the mixture filtered. Addition of 60 mL of Et_2O followed by agitation produced black crystals. The solution was cooled at 0 °C overnight and then for 2 h at −78 °C. The product was isolated by filtration, washed thoroughly with 10 mL of MeOH, washed with Et_2O, and dried

(4) Kolis, J. W.; Holt, E. M.; Shriver, D. F. *J. Am. Chem. Soc.* **1983**, *105*, 7307.
(5) Hriljac, J. A.; Shriver, D. F. *J. Am. Chem. Soc.* **1987**, *109*, 6010.
(6) Sailor, M. J.; Brock, C. P.; Shriver, D. F. *J. Am. Chem. Soc.* **1987**, *109*, 6015.
(7) Went, M. J.; Sailor, M. J.; Bogdan, P. L.; Brock, C. P.; Shriver, D. F. *J. Am. Chem. Soc.* **1987**, *109*, 6023.
(8) Ching, S.; Sabat, M.; Shriver, D. F. *J. Am. Chem. Soc.* **1987**, *109*, 4722.
(9) Shriver, D. F.; Drezdzon, M. A. *The Manipulation of Air-Sensitive Compounds*, 2nd ed.; Wiley: New York, 1986.

under vacuum. Yield: 1.88 g (87%). IR (CH_2Cl_2): ν_{CO} 2003 (w), 1939 (s), 1912 (m, sh) cm^{-1}. ^1H NMR (CD_2Cl_2, +25 °C): 2.31 (m, 1 H, CH_AH_B), 1.90 (m, 1 H, CH_AH_B), 1.61 (d, 3 H, $^2J_{PH}$ = 8.0 Hz, CH_3), 1.49 (d, 3 H, $^2J_{PH}$ = 8.0 Hz, CH_3), 1.48 (d, 3 H, overlapping with 1.49 ppm resonance, $^2J_{PH}$ = 8.0 Hz, CH_3), 1.39 (d, 3 H, $^2J_{PH}$ = 8.0 Hz, CH_3) ppm. ^{31}P NMR (CD_2Cl_2, -90 °C) second-order: 44.1 (d, Fe–P), 26.3 (d, Co–P) ppm, $J_{PP}(AB)$ = 77.0 Hz. Anal. Calcd for $C_{51}H_{46}Cl_2CoFe_2NO_8P_4$: C, 52.46; H, 3.94; P, 10.63; Fe, 9.58; Co, 5.05. Found: C, 52.65; H, 4.05; P, 11.31; Fe, 9.42; Co, 5.01.

$Fe_2Co(CO)_8(dmpm)(CH)$ (7). A 0.10-g (0.086-mmol) sample of [PPN][$Fe_2Co(CO)_7$(dmpm)(CCO)]·CH_2Cl_2 was dissolved in 4 mL of CH_2Cl_2, and 10 μL (0.11 mmol) of HSO_3CF_3 was added with stirring. An immediate color change to purple was observed, and after 5 min the solution was passed down a column of Florisil and eluted with CH_2Cl_2. A purple band was collected, and the solution was concentrated to ca. 1 mL under vacuum. The solution was layered with 4 mL of hexane and cooled at 0 °C overnight. Purple crystals were isolated by filtration, washed with hexane, and dried under vacuum. Yield: 0.04 g (74%). IR: (CH_2Cl_2) ν_{CO} 2052 (m), 1997 (s), 1915 (m, sh), 1889 (w), 1805 (w) cm^{-1}. MS: parent ion m/e 544 with successive loss of eight CO units. ^1H NMR (CD_2Cl_2, +25 °C): 12.16 (dd, 1 H, $J_{P(A)H}$ = 13.7 Hz, $J_{P(B)H}$ = 4.1 Hz, μ_3-CH), 2.67 (m, 1 H, CH_AH_B), 2.08 (m, 1 H, partially obscured by 2.06 ppm resonance, CH_AH_B), 2.06 (d, 3 H, $^2J_{PH}$ = 9.6 Hz, CH_3), 1.75 (d, 3 H, $^2J_{PH}$ = 9.2 Hz, CH_3), 1.58 (d, 3 H, $^2J_{PH}$ = 8.0 Hz, CH_3), 1.29 (d, 3 H, $^2J_{PH}$ = 8.8 Hz,. CH_3) ppm. ^{31}P NMR (CD_2Cl_2, -90 °C) second-order: 52.7 (d, Fe–P), 29.2 (br, Co–P) ppm, $J_{PP}(AB)$ = 77.0 Hz. Anal. Calcd for $C_{14}H_{15}CoFe_2O_8P_2$: C, 30.92; H, 2.76. Found: C, 31.75; H, 3.08.

$Fe_2Co(CO)_8(dmpm)(CCH_3)$ (8). A 0.25-g (0.21-mmol) sample of [PPN][$Fe_2Co(CO)_7$(dmpm)(CCO)]·CH_2Cl_2 was dissolved in 6 mL of CH_2Cl_2 and treated with 0.30 mL (4.8 mmol) of CH_3I. After 2 h of stirring, the solution became red and the solvent and excess CH_3I were removed under vacuum. The resulting oil was extracted in 16 mL of Et_2O and filtered to remove [PPN]I. The solvent was removed under vacuum, and the resulting oil was dissolved in 4 mL of CH_2Cl_2 and then passed down a column of Florisil. Elution with CH_2Cl_2/hexane (1:1) produced a single purple-red band which was collected before the solvent was removed under vacuum. The product was dissolved in 2 mL of CH_2Cl_2, layered with 10 mL of pentane, and cooled at 0 °C overnight. Black crystals were isolated by filtration, washed with pentane, and vacuum dried. Yield: 0.06 g (50%). IR: (CH_2Cl_2) ν_{CO} 2051 (m), 1993 (s), 1962 (m), 1935 (w), 1798 (w) cm^{-1}. MS: parent ion m/e 558 with successive loss of eight CO units; ^1H NMR (CD_2Cl_2, +25 °C): 4.25 (d, 3 H, J_{PH} = 5.6 Hz, μ_3-CCH_3), 2.80 (m, 1 H, CH_AH_B), 2.29 (m, 1 H, CH_AH_B), 1.83 (d, 3 H, $^2J_{PH}$ = 9.2 Hz, CH_3), 1.72 (d, 3 H, $^2J_{PH}$ = 8.8 Hz, CH_3), 1.53 (d, 3 H, $^2J_{PH}$ = 8.0 Hz, CH_3), 1.38 (d, 3 H, $^2J_{PH}$ = 8.4 Hz, CH_3) ppm. ^{31}P NMR (CD_2Cl_2, -90 °C) second-order: 48.5 (d, Fe–P), 25.1 (d, Co–P) ppm, $J_{PP}(AB)$ = 70.8 Hz. Anal. Calcd for $C_{15}H_{17}CoFe_2O_8P_2$: C, 32.28; H, 3.05. Found: C, 33.12; H, 3.09.

$Fe_2Co(CO)_7(dmpm)(CCOCH_3)$ (9). A 0.10-g (0.086-mmol) sample of [PPN][$Fe_2Co(CO)_7$(dmpm)(CCO)]·CH_2Cl_2 was dissolved in 6 mL of CH_2Cl_2 and treated with 20 μL (0.018 mmol) of $CH_3SO_3CF_3$. After 40 min of stirring, the solution became brown and the solvent was removed under vacuum. The resulting oil was extracted with 8 mL of Et_2O and filtered to remove [PPN][SO_3CF_3]. The solvent was removed under vacuum, and 1.5 mL of CH_2Cl_2 was added to dissolve the oil. The solution was passed down a column of Florisil and eluted with CH_2Cl_2/hexane (1:1.5). A brown band was collected as a purple-red band of $Fe_2Co(CO)_8(dmpm)(CCH_3)$ remained at the top of the column. The solvent was removed under vacuum, and the solid was redissolved in 1 mL of CH_2Cl_2, layered with 4 mL of pentane, and cooled at 0 °C overnight. Black crystals were isolated by filtration, washed with pentane, and vacuum dried. Yield: 0.02 g (42%). IR: (CH_2Cl_2) ν_{CO} 2038 (w), 1980 (s), 1960 (m), 1911 (w) cm^{-1}. MS: parent ion m/e 558 with successive loss of seven CO units. ^1H NMR (CD_2Cl_2, +25 °C): 3.95 (s, 3 H, OCH_3), 2.51 (m, 1 H, CH_AH_B), 2.04 (m, 1 H, CH_AH_B), 1.78 (d, 3 H, $^2J_{PH}$ = 9.6 Hz, CH_3), 1.60 (d, 3 H, $^2J_{PH}$ = 9.2, CH_3), 1.46 (d, 3 H, overlapped with 1.44 ppm resonance, $^2J_{PH}$ = 8.8 Hz, CH_3), 1.44 (d, 3 H, $^2J_{PH}$ = 8.0 Hz, CH_3) ppm. ^{31}P NMR (CD_2Cl_2, -90 °C) second-order: 47.2 (d, Fe–P), 20.9 (br, Co–P) ppm, $J_{PP}(AB)$ = 64.7 Hz. Anal. Calcd for $C_{15}H_{17}CoFe_2O_8P_2$: C, 32.28; H, 3.05. Found: C, 32.46; H, 3.04.

Table I. Crystal Data for [PPN][$Fe_2Co(CO)_9(CPMe_3)$] (3a) and [PPN][$Fe_2Co(CO)_7$(dmpm)(CCO)]•CH_2Cl_2 (6•CH_2Cl_2)

	3a	6·CH_2Cl_2
formula	$C_{49}H_{39}CoFe_2NO_9P_3$	$C_{50}H_{44}CoFe_2NO_8P_4$, CH_2Cl_2
M	1049.40	1166.35
cryst size, mm	0.38 × 0.32 × 0.28	0.43 × 0.36 × 0.20
cryst system	monoclinic	triclinic
space group	$P2_1/c$	$P\bar{1}$
a, Å	14.370 (3)	16.398 (2)
b, Å	18.761 (2)	16.858 (2)
c, Å	17.621 (3)	9.478 (2)
α, deg	90.0	94.89 (1)
β, deg	94.21 (2)	99.11 (1)
γ, deg	90.0	93.06 (1)
V, Å^3	4738 (2)	2572 (1)
Z	4	2
d_{calcd}, g·cm^{-3}	1.47	1.51
μ(Mo Kα), cm^{-1}	11.39	11.84
radiatn	graphite-monochromated Mo Kα (λ = 0.71069 Å)	
scan type	$\theta/2\theta$	
2θ range, deg	4–50	4–45
unique data	8584	6699
unique data with $I > 3\sigma(I)$	5969	5456
no. of parameters	586	622
$R(F)$	0.034	0.035
$R_w(F)$	0.046	0.058
GOF	1.57	1.73

[PPN][$Fe_2Co(CO)_8(PR_3)$(CCO)] (2a–f) and [PPN][$Fe_2Co(CO)_9(CPR_3)$] (3b–e) Clusters. The specific formulas of PR_3 and the corresponding lettering scheme for these compounds are given in Scheme I. The clusters were generated and studied in solution without isolation. A typical reaction required 0.05 g (0.05 mmol) of [PPN][$Fe_2Co(CO)_9$(CCO)] to be dissolved in 4 mL of CH_2Cl_2 and treated with 2–10 equiv of the appropriate phosphine or phosphite ligand.

X-ray Crystal Structures of [PPN][$Fe_2Co(CO)_9(CPMe_3)$] (3a) and [PPN][$Fe_2Co(CO)_7$(dmpm)(CCO)]·CH_2Cl_2 (6·CH_2Cl_2). Crystallographic data for compounds **3a** and **6** are summarized in Table I. Dark red crystals of **3a** suitable for analysis were grown by slow cooling of a saturated MeOH solution. Purple-black crystals of **6** were grown by slow diffusion of Et_2O into a 1:1 CH_2Cl_2/Et_2O solution of the cluster. Each crystal was mounted on a glass fiber and transferred to a N_2 cold stream (-120 °C) of an Enraf-Nonius CAD4 diffractometer. All measurements were performed by using Mo Kα radiation (λ = 0.71069 Å). Lattice parameters were determined by the least-squares refinement of the setting angles of 25 independent reflections. Intensities of three standard reflections were measured every 3 h of X-ray exposure and showed no significant changes. The data were corrected for Lorentz and polarization effects. Empirical absorption corrections were applied on the basis of Ψ scans of six Bragg reflections.

The structure of **3a** was solved by direct methods using the MULTAN program of the SDP package[10] and refined by using TEXSAN 2.0 crystallographic software:[11] Direct methods (MITHRIL)[12] were also applied to the structure solution of **6** with refinement done using TEXSAN 2.0. Full-matrix least-squares refinement initially with isotropic and then with anisotropic thermal parameters for all non-hydrogen atoms led to the final R values of 0.034 (R_w = 0.046) for **3a** and 0.035 (R_2 = 0.058) for **6**. The goodness-of-fit was 1.57 and 1.73 for **3a** and **6**, respectively. The final difference Fourier map showed no significant residual peaks for **3a**, with the largest one being 0.46 e/Å^3. The difference

(10) SDP B. A. Frenz and Assoc., College Station, TX, and Enraf-Nonius, Delft, Holland, 1985.
(11) Swepston, P. N. TEXSAN, Version 2.0; the TEXRAY Structure Analysis Program Package, Molecular Structure Corp., College Station, TX, 1986.
(12) Gilmore, G. N. MITHRIL, A computer program for the automatic solution of crystal structures from X-ray data; University of Glasgow: Glasgow, Scotland, 1983.

Table II. Positional Parameters for the Cluster Anion of $[PPN][Fe_2Co(CO)_9(CPMe_3)]$ (3a)

atom	x	y	z
Co1	0.71028 (3)	0.09908 (2)	0.15424 (2)
Fe2	0.86632 (3)	0.16363 (2)	0.15656 (3)
Fe3	0.72617 (3)	0.20876 (2)	0.07234 (2)
P1	0.71709 (6)	0.24934 (4)	0.25356 (5)
C1	0.7435 (2)	0.1955 (2)	0.1795 (2)
C2	0.7551 (3)	0.2132 (2)	0.3446 (2)
C3	0.7681 (3)	0.3364 (2)	0.2491 (2)
C4	0.5939 (3)	0.2626 (3)	0.2563 (2)
C11	0.7341 (2)	0.0475 (2)	0.2369 (2)
C12	0.7178 (3)	0.0301 (2)	0.0834 (2)
C13	0.5889 (3)	0.1012 (2)	0.1569 (2)
C21	0.9298 (3)	0.2436 (2)	0.1508 (3)
C22	0.9123 (2)	0.1285 (2)	0.2450 (2)
C23	0.9065 (2)	0.1036 (2)	0.0873 (2)
C31	0.7338 (2)	0.1556 (2)	−0.0112 (2)
C32	0.7761 (3)	0.2894 (2)	0.0461 (2)
C33	0.6111 (3)	0.2399 (2)	0.0611 (2)
O11	0.7480 (2)	0.0120 (1)	0.2902 (1)
O12	0.7218 (2)	−0.0147 (1)	0.0403 (1)
O13	0.5095 (2)	0.1023 (1)	0.1607 (2)
O21	0.9710 (2)	0.2961 (2)	0.1486 (3)
O22	0.9414 (2)	0.1063 (2)	0.3026 (2)
O23	0.9336 (2)	0.0643 (1)	0.0443 (1)
O31	0.7368 (2)	0.1227 (1)	−0.0658 (1)
O32	0.8064 (3)	0.3427 (2)	0.0266 (2)
O33	0.5359 (2)	0.2623 (2)	0.0543 (2)

Table III. Positional Parameters for the Cluster Anion of $[PPN][Fe_2Co(CO)_7(dmpm)(CCO)]\bullet CH_2Cl_2$ ($6\bullet CH_2Cl_2$)

atom	x	y	z
Co	0.80747 (3)	0.27680 (3)	0.46282 (5)
Fe1	0.70026 (3)	0.15683 (3)	0.41115 (5)
Fe2	0.72345 (4)	0.24390 (3)	0.21391 (6)
P1	0.80388 (6)	0.29513 (6)	0.6925 (1)
P2	0.69403 (6)	0.14430 (6)	0.6370 (1)
O1	0.5483 (3)	0.2803 (3)	0.4204 (7)
O11	0.8722 (2)	0.4373 (2)	0.4349 (3)
O12	0.9594 (2)	0.1960 (2)	0.4526 (3)
O21	0.8275 (2)	0.0460 (2)	0.3811 (4)
O22	0.5498 (2)	0.0616 (2)	0.2817 (4)
O31	0.5767 (2)	0.1796 (2)	0.0140 (4)
O32	0.7491 (2)	0.3953 (2)	0.0942 (3)
O33	0.8514 (2)	0.1501 (2)	0.1107 (3)
C1	0.6917 (2)	0.2737 (2)	0.4003 (5)
C2	0.6180 (3)	0.2721 (3)	0.4083 (6)
C3	0.7921 (3)	0.3982 (3)	0.7594 (5)
C4	0.8894 (3)	0.2704 (3)	0.8207 (5)
C5	0.7668 (3)	0.0808 (3)	0.7291 (5)
C6	0.5958 (3)	0.1081 (3)	0.6820 (5)
C7	0.7152 (2)	0.2410 (2)	0.7438 (4)
C11	0.8458 (2)	0.3735 (3)	0.4433 (4)
C12	0.8986 (3)	0.2269 (2)	0.4575 (4)
C21	0.7782 (3)	0.0911 (2)	0.3920 (4)
C22	0.6095 (3)	0.0998 (2)	0.3304 (4)
C31	0.6347 (3)	0.2049 (3)	0.0943 (4)
C32	0.7400 (3)	0.3355 (3)	0.1419 (4)
C33	0.8018 (3)	0.1871 (2)	0.1537 (4)

map of 6 contained a large residual peak of 1.31 e/Å^3, but this peak was located near one of the chlorine atoms of the CH_2Cl_2 solvent molecule. Atomic scattering factors were those tabulated by Cromer and Waber[13a] with anomalous dispersion corrections taken from the literature.[13b] All calculations were performed on a VAX 11/730 computer. Final coordinates for all non-hydrogen atoms of the cluster anions of **3a** and **6** are reported in Tables II and III, respectively.

Results and Discussion

Formation and Characterization of $[Fe_2Co(CO)_8(PR_3)(CCO)]^-$ and $[Fe_2Co(CO)_9(CPR_3)]^-$ Clusters. The reaction that was previously reported for $[PPN][Fe_2Co(CO)_9(CCO)]$ (1) and PMe_3[8] has been extended to other simple phosphines and phosphites (Scheme I) and the same general reaction pathway is observed in almost all instances. Initial ligand substitution for CO occurs at the Co metal center of 1, and this is followed by an apparent migration of the phosphine ligand to the capping carbon atom. The CO group of the ketenylidene ligand is displaced onto the metal framework as the ylide group forms. The reaction sequence in Scheme I appears to be general for phosphines with relatively small cone angles,[14] although in the case of $P(OPh)_3$ only the substitution step is observed. Bulky phosphines such as PPh_3 and $P(C_6H_{11})_3$ do not react with 1. All of the phosphine-substituted clusters were characterized spectroscopically in solution, and only $[PPN][Fe_2Co(CO)_9(CPMe_3)]$ (**3a**) was isolated in crystalline form.

The intermediate cluster compounds $[PPN][Fe_2Co(CO)_8(PR_3)(CCO)]$ (**2a–e**) could be observed in solution since their formation is rapid compared to subsequent isomerization to **3a–e**. Cluster **2f** does not isomerize. Infrared data in the ν_{CO} region and NMR data for **2a–f** are presented in Tables IV and V, respectively. The IR bands and ^1H NMR resonances were obtained during the course of reaction at room temperature whereas ^{31}P and ^{13}C NMR resonances were obtained from samples which were quenched at −90 °C after $[Fe_2Co(CO)_8(PR_3)(CCO)]^-$ became the dominant species in solution. The structure of compounds **2a–f** is believed to be one in which PR_3 has selectively substituted for CO at one of the equatorial positions of the Co metal center. The selectivity of

Scheme I

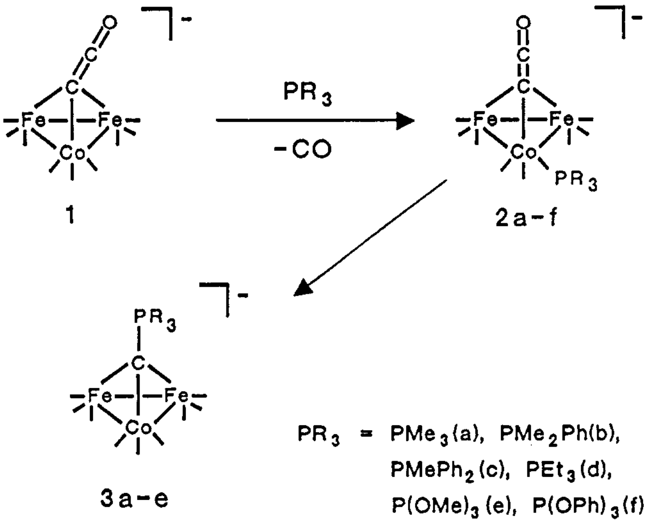

Table IV. IR Data (ν_{CO})[a] for PR_3-Substituted $[PPN][Fe_2Co(CO)_9(CCO)]$ Clusters

PR_3	$[PPN][Fe_2Co(CO)_8(PR_3)(CCO)]$[b]	$[PPN][Fe_2Co(CO)_9(CPR_3)]$
PMe_3	2037 (w), 1964 (s)	2023 (w), 1988 (m), 1952 (s), 1901 (m)
PMe_2Ph	2037 (w), 1966 (s)	2023 (w), 1953 (s), 1901 (m)
$PMePh_2$	2039 (w), 1968 (s)	2021 (w), 1954 (s), 1899 (m)
PEt_3	2035 (w), 1965 (s)	2021 (w), 1949 (s), 1901 (m)
$P(OMe)_3$	2046 (w), 1977 (s)	2027 (w), 2002 (m, sh), 1958 (s), 1948 (s, sh)
$P(OPh)_3$	2049 (w), 1980 (s)	

[a] ν_{CO} reported in cm^{-1} and recorded in CH_2Cl_2 solution. [b] Only the highest intensity and highest ν_{CO} bands reported.

(13) (a) *International Tables for X-ray Crystallography*; Kynoch: Birmingham, England, 1974; Vol. 14, p 99. (b) Ibid, p 149.

(14) Tolman, C. A. *Chem. Rev.* **1977**, *77*, 313.

Table V. NMR Data for [PPN][$Fe_2Co(CO)_8(PR_3)(CCO)$] Clusters[a,b]

PR_3	^1H (+25 °C)[c]	^{31}P (−90 °C)[d]	^{13}C (−90 °C)[c,f]
PMe_3	1.37 (d, J_{PH} = 8.6 Hz)	2.0	216.1 (CO), 177.1 (CCO), 86.4 (CCO); $^1J_{CC}$ = 73.3 Hz
PMe_2Ph	1.66 (d, J_{PH} = 7.9 Hz, CH_3), 7.9–7.3 (m, Ph)[e]	16.0	216.0 (CO); 176.7 (CCO), 86.4 (CCO); $^1J_{CC}$ = 69.7 Hz
$PMePh_2$	1.93 (d, J_{PH} = 7.9 Hz, CH_3), 7.5–7.3 (m, Ph)[e]	30.3	216.2 (CO), 175.0 (CCO), 84.0 (CCO); $^1J_{CC}$ = 73.8 Hz
PEt_3	1.81 (m, CH_2), 1.18 (m, CH_3)	32.0	216.1 (CO), 183.7 (CCO), 95.7 (CCO); $^1J_{CC}$ = 69.0 Hz
$P(OMe)_3$	3.57 (d, J_{PH} = 11.7 Hz)	175.9	215.6 (CO), 185.0 (CCO), 97.1 (CCO); $^1J_{CC}$ = 66.1 Hz
$P(OPh)_3$	7.4–7.0 (m)[e]	161.4	217.0 (6CO), 208.2 (2CO), 177.0 (CCO), 90.9 (CCO); $^1J_{CC}$ = 73.0 Hz

[a] Generated in CD_2Cl_2 solution. Signals due to PPN^+ are not reported. [b] All resonances singlets unless noted: d, doublet; m, multiplet; ds, doublet on singlet. [c] Chemical shifts in ppm relative to TMS. [d] Chemical shifts in ppm relative to 85% H_3PO_4. [e] Overlapping with PPN^+. [f] $^1J_{CC}$ obtained from CCO resonance (ds).

Table VI. ^{59}Co NMR Data for Trimetallic Fe_2Co Clusters[a]

compound	δ,[b] ppm	$\Delta\nu_{1/2}$, Hz
[PPN][$Fe_2Co(CO)_9(CCO)$]	−2670	250
[PPN][$Fe_2Co(CO)_9(CPMe_3)$]	−2470	1800
[PPN][$Fe_2Co(CO)_9(CPMe_2Ph)$]	−2450	2500
[PPN][$Fe_2Co(CO)_9(CPEt_3)$]	−2460	2500
[PPN][$Fe_2Co(CO)_9(CP(OMe)_3)$]	−2370	1300
[PPN][$Fe_2Co(CO)_8(PMe_2Ph)(CCO)$]	−1510	2400
[PPN][$Fe_2Co(CO)_8(PEt_3)(CCO)$]	−1560	2600
[PPN][$Fe_2Co(CO)_8(P(OMe)_3)(CCO)$]	−1900	2600

[a] $(CD_3)_2CO$, +25 °C. [b] Shifts reported relative to saturated $K_3Co(CN)_6$ in D_2O.

phosphines for Co over Fe atoms is not easily explained, but empirically this phenomenon is well precedented in mixed-metal compounds.[15–17] Evidence for phosphine coordination to the Co atom was obtained from multinuclear NMR spectroscopy. The ^{31}P NMR spectra of **2a–f** recorded at −90 °C exhibit broad resonances that become increasingly broader as the temperature is raised. Such behavior is consistent with partial coupling of the phosphorus atom to the quadrupolar ^{59}Co nucleus. Phosphine coordination to the Co metal center is also indicated by ^{59}Co NMR data of some selected clusters (Table VI). The resonances fall in the expected range of low-valent Co compounds,[18] with **1** having the most shielded resonance at −2670 ppm. Clusters **2b, 2d,** and **2e** exhibit characteristic resonances that are significantly deshielded ($\Delta\delta$ = 770–1160 ppm) relative to **1**. By contrast, ligand substitution at an atom adjacent to the Co vertex, such as in the ylide-capped clusters, produces a shift of only 200–300 ppm toward more deshielded resonances. The ^{13}C NMR spectra of **2a–e** recorded at −90 °C exhibit characteristic features of ketenylidene clusters (Table V). All metal-bonded carbonyl ligands are represented by a single resonance near 216 ppm while resonances due to the carbonyl carbon and capping carbon atoms of the CCO ligand appear in the regions from 175 to 185 and 80 to 100 ppm, respectively. These resonances are deshielded in comparison to those of **1**[3] and shifted in the proper direction for clusters that have become more electron rich.[19] The spectrum of **2f** recorded at −90 °C is similar to those of **2a–e**, except that two resonances are observed in the terminal carbonyl region. Variable-temperature ^{13}C NMR spectra of **2f** recorded down to a low temperature of −130 °C are consistent with phosphine coordination to the Co atom in an equatorial position (Figure 1 and Table VII). At −60 °C, complete intermetallic exchange equilibrates all eight CO ligands on the metal framework and a single resonance is observed. Cooling to −90 °C interrupts intermetallic ex-

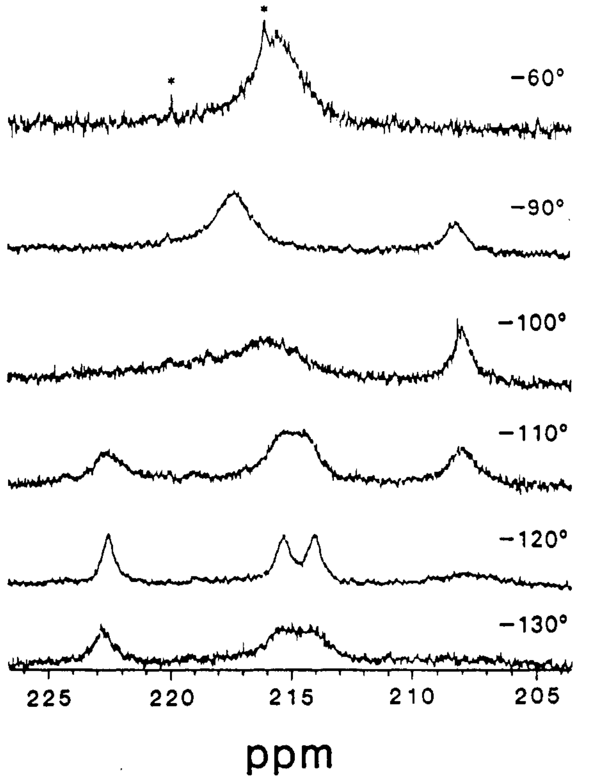

Figure 1. Variable-temperature ^{13}C NMR spectra (100.577 MHz) of the carbonyl region of [PPN][$Fe_2Co(CO)_8(P(OPh)_3)(CCO)$] (**2f**) recorded in 1:2 $CD_2Cl_2/CHFCl_2$. Peaks due to minor impurities are marked with an asterisk.

Table VII. Variable-Temperature ^{13}C NMR Data for CCO-Containing Clusters[a,b]

compound	temp, °C	^{13}C NMR,[c] ppm
[PPN][$Fe_2Co(CO)_8(P(OPh)_3)$-(CCO)] (**2f**)	−60	215.6
	−90	217.4 (6), 208.3 (2)
	−120	222.7 (2), 215.4 (2), 214.2 (2)
[PPN][$Fe_2Co(CO)_8(P(OMe)_3)$-(CCO)] (**2e**)	−80	215.9
	−130	222.3 (2), 214.4 (2), 213.3 (2), 209.5 (2)
[PPN][$Fe_2Co(CO)_8(PEt_3)(CCO)$] (**2d**)	−90	216.7
	−130	223.2 (2), 215.1 (br, 4), 212.4 (2)
[PPN][$Fe_2Co(CO)_9(CCO)$] (**1**)	−130	222.2 (2), 215.3 (2), 212.5 (2), 204.6 (3)

[a] 1:2 mixture of $CD_2Cl_2/CHFCl_2$. [b] Resonances due to CCO and PPN^+ are not listed. [c] Numbers in parentheses are relative intensities.

(15) Aime, S.; Milone, L.; Rossetti, R.; Stanghellini, P. L. *Inorg. Chim. Acta* **1977**, *25*, 103.
(16) (a) Cooke, C. G.; Mays, M. J. *J. Organomet. Chem.* **1974**, *74*, 449. (b) Huie, B. T.; Knobler, C. B.; Kaesz, H. D. *J. Am. Chem. Soc.* **1978**, *100*, 3059. (c) Langenbach, H.-J.; Vahrenkamp, H. *Chem. Ber.* **1979**, *112*, 3390. (d) Low, A. A.; Lauher, J. W. *Inorg. Chem.* **1987**, *26*, 3863.
(17) Albiez, T.; Vahrenkamp, H. *Angew. Chem., Int. Ed. Engl.* **1987**, *26*, 572.
(18) (a) Lucken, E. A. C.; Noack, K.; Williams, D. F. *J. Chem. Soc. A* **1967**, 148. (b) Speiss, H. W.; Sheline, R. K. *J. Chem. Phys.* **1970**, *53*, 3036.
(19) Chini, P.; Heaton, B. T. *Top. Curr. Chem.* **1977**, *71*, 1.

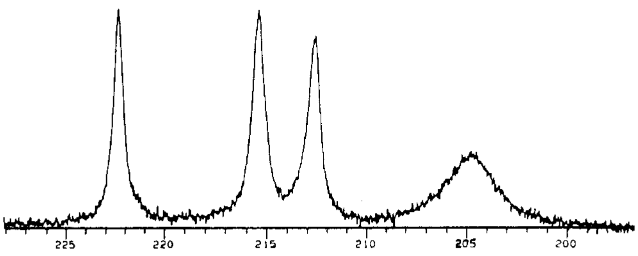

Figure 2. ^{13}C NMR spectrum (100.577 MHz) of the carbonyl region of [PPN][$Fe_2Co(CO)_9(CCO)$] recorded (1) at -130 °C in 1:2 $CD_2Cl_2/CHFCl_2$.

change, but localized exchange at each metal vertex is still rapid. The result is a 6:2 pattern due to a pair of equivalent $Fe(CO)_3$ groups and one $Co(CO)_2(P(OPh)_3)$ group. At -120 °C, localized CO exchange at each Fe vertex freezes out and results in a splitting of the peak at 217.4 ppm into a 2:2:2 pattern for two axial (222.7 ppm) and four equatorial (215.4 and 214.2 ppm) carbonyl ligands.[15] The $Co(CO)_2(P(OPh)_3$ resonance at 203.8 ppm broadens but remains fluxional, thus preserving C_s symmetry in the cluster. At -130 °C all resonances broaden as the peak at 203.8 ppm coalesces, thus reflecting a transition in the molecular symmetry from C_s to C_1 as the two carbonyl ligands on the Co atom freeze out into axial and equatorial positions. Similar variable-temperature behavior is observed for ^{13}C NMR spectra of **2d** and **2e** although coalescence resulting from the transition from C_s to C_1 symmetry is not observed down to the lowest temperature investigated, -130 °C. In the interpretation of the spectra displayed in Figure 1, it is assumed that the CCO ligand of [$Fe_2Co(CO)_8(PR_3)(CCO)]^-$ clusters either is perpendicular to the plane of the metal triangle or, if tilted, undergoes a rapid, low-energy precession about the metal framework.[7,20]

The substitution of a phosphine ligand for CO on **1** appears to have only a slight affect on the fluxionality of the remaining carbonyl ligands around the metal framework. The ^{13}C NMR spectrum of **1** recorded at -90 °C has previously been reported,[3] but the spectrum recorded at -130 °C is given here (Figure 2, Table VII) for comparison with **2d–f**. The spectrum of **1** is correct for C_s symmetry in solution (the solid-state structure has a tilted CCO ligand and C_1 symmetry), with three deshielded resonances assigned to CO ligands of two symmetry-related $Fe(CO)_3$ vertices and a broader, shielded resonance due to the fluxional carbonyl ligands of the $Co(CO)_3$ vertex. Similar spectral features are observed for **2d–f** at or near the lowest temperatures investigated (Table VII). A qualitative comparison of these spectra suggests that **1** and **2d–f** do not differ greatly in their activation energies for intramolecular carbonyl exchange.

The ylide-capped clusters [PPN][$Fe_2Co(CO)_9(CPR_3)$] (**3a–e**) have been characterized by IR (Table IV) and NMR (Table VIII) spectroscopies and, in the case of **3a**, by a single-crystal X-ray diffraction study. The ^{13}C NMR spectra of these clusters are particularly diagnostic for the μ_3-CPR_3 ligand. The resonance of the capping carbon atom is typically a doublet in the region from 190 to 205 ppm when bonded to a phosphine ligand, although attachment of $P(OMe)_3$ gives a doublet at 159 ppm. One-bond coupling between phosphorus and the capping carbon atom ranges from 19 to 34 Hz except for $P(OMe)_3$, which exhibits 113-Hz coupling. The $^1J_{PC}$ values for compounds **3a–d** are low in comparison with organic ylides,[21] but $^1J_{PC}$ of phosphorus ylides in organometallic compounds are known to exhibit a wide range of values.[22] Terminally bonded M≡C—PR_3 ylide groups, which are the mononuclear analogs to the cluster-bound ylides **3a–e**, show no observable phosphorus–carbon coupling.[23,24]

A single-crystal X-ray diffraction study was performed on [PPN][$Fe_2Co(CO)_9(CPMe_3)$] (**3a**), and the molecular

Table VIII. NMR Data for [PPN][$Fe_2Co(CO)_9(CPR_3)$] Clusters[a,b]

PR_3	^1H (+25 °C)[c]	^{31}P (-90 °C)[d]	^{13}C (-90 °C)[c,f]
PMe_3	1.84 (d, J_{PH} = 11.9 Hz)	24.6	217.1 (CO), 203.3 ($^1J_{PC}$ = 33.5 Hz)
PMe_2Ph	2.16 (d, J_{PH} = 11.9 Hz, CH_3), 7.9–7.3 (m, Ph)[e]	27.4	216.9 (CO), 202.2 ($^1J_{PC}$ = 25.4 Hz)
$PMePh_2$	2.45 (d, J_{PH} = 12.5 Hz, CH_3), 7.5–7.3 (m, Ph)[e]	25.2	217.4 (CO), 192.4 ($^1J_{PC}$ = 19.1 Hz)
PEt_3	2.13 (m, CH_2), 1.30 (m, CH_3)	42.7	217.0 (CO), 193.6 ($^1J_{PC}$ = 21.4 Hz)
$P(OMe)_3$	3.89 (d, J_{PH} = 10.3 Hz)	59.2	216.5 (CO), 159.3 ($^1J_{PC}$ = 113.7 Hz)

[a] CD_2Cl_2 solution. Signals due to PPN^+ are not reported. [b] All resonances are singlets unless noted: d, doublet; m, multiplet. [c] Chemical shifts in ppm relative to TMS. [d] Chemical shifts in ppm relative to 85% H_3PO_4. [e] Overlapping with PPN^+. [f] More shielded resonance is a doublet due to μ_3-C.

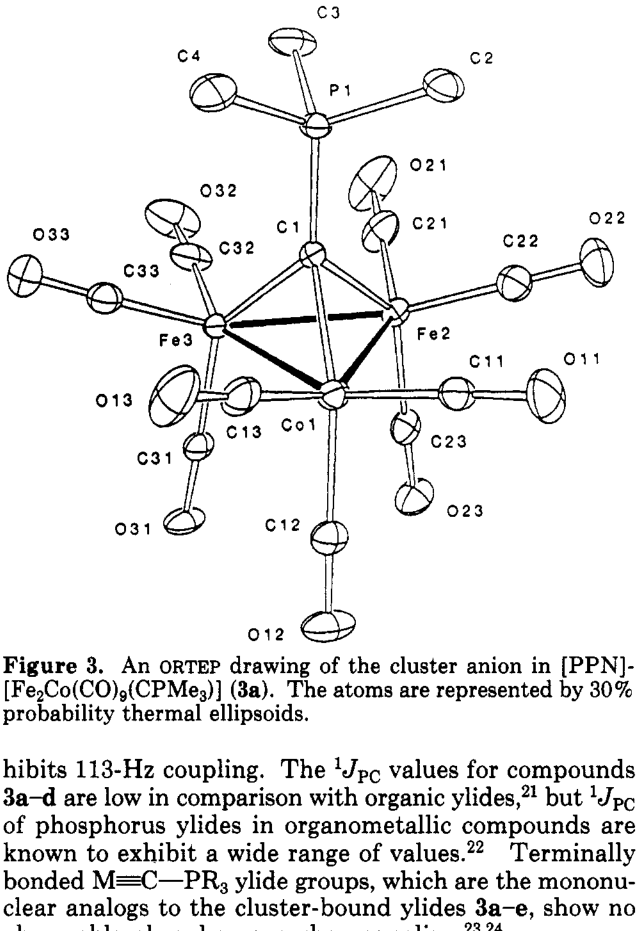

Figure 3. An ORTEP drawing of the cluster anion in [PPN]-[$Fe_2Co(CO)_9(CPMe_3)$] (**3a**). The atoms are represented by 30% probability thermal ellipsoids.

(20) D'Agostino, M. F.; Mlekuz, M.; Kolis, J. W.; Sayer, B. G.; Rodger, C. A.; Halet, J.-F.; Saillard, J.-Y.; McGlinchey, M. J. *Organometallics* **1986**, *5*, 2345.

(21) (a) Schmidbaur, H.; Richter, W.; Wolf, W.; Köhler, F. H. *Chem. Ber.* **1975**, *108*, 2649. (b) Albright, T. A.; Freeman, W. J.; Schweizer, E. E. *J. Am. Chem. Soc.* **1975**, *97*, 940.

(22) For reviews of phosphorus ylides in organometallic compounds, see: (a) Schmidbaur, H. *Angew. Chem., Int. Ed. Engl.* **1983**, *22*, 907. (b) Kaska, W. C. *Coord. Chem. Rev.* **1983**, *48*, 1.

(23) Holmes, S. J.; Schrock. R. R.; Churchill, M. R.; Wasserman, H. J. *Organometallics* **1984**, *3*, 475.

(24) Bruce, A. E.; Gamble, A. S.; Tonker, T. L.; Templeton, J. L. *Organometallics* **1987**, *6*, 1350.

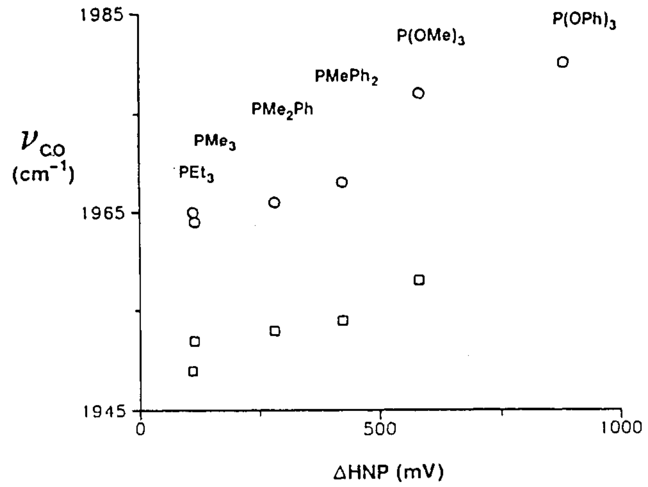

Figure 4. Relationship between ν_{CO} and phosphine basicity for $[Fe_2Co(CO)_8(PR_3)(CCO)]^-$ (circles) and $[Fe_2Co(CO)_9(CPR_3)]^-$ (squares) clusters. Values of ΔHNP are inversely related to basicity and listed in ref 30.

Table IX. Selected Bond Distances (Å) and Angles (deg) for [PPN][Fe$_2$Co(CO)$_9$(CPMe$_3$)] (3a)

Bond Distances			
Co1–Fe2	2.546 (1)	Fe3–C1	1.903 (3)
Co1–Fe3	2.533 (1)	P1–C1	1.715 (3)
Fe2–Fe3	2.557 (1)	P1–C2	1.790 (4)
Co1–C1	1.914 (3)	P1–C3	1.795 (4)
Fe2–C1	1.934 (3)	P1–C4	1.791 (4)
Bond Angles			
Co1–Fe2–Fe3	59.53 (2)	C1–P1–C4	112.1 (2)
Co1–Fe3–Fe2	60.03 (2)	C2–P1–C3	106.6 (2)
Fe2–Co1–Fe3	60.44 (2)	C2–P1–C4	105.4 (2)
Co1–C1–Fe2	82.8 (1)	C3–P1–C4	106.4 (2)
Co1–C1–Fe3	83.2 (1)	C1–Co1–C12	144.2 (1)
Fe2–C1–Fe3	83.6 (1)	C1–Fe2–C23	133.1 (1)
Co1–C1–P1	132.0 (2)	C1–Fe3–C31	137.1 (1)
Fe2–C1–P1	126.7 (2)	C11–Co1–C13	97.1 (2)
Fe3–C1–P1	131.1 (2)	C21–Fe2–C22	101.9 (2)
C1–P1–C2	112.9 (2)	C32–Fe3–C33	94.8 (2)
C1–P1–C3	112.9 (2)		

structure of the anionic cluster is shown in Figure 3. The $M_3(CO)_9$ portion of the molecule is similar to that of the starting material **1**[3] and contains six equatorial and three axial carbonyl ligands. The μ_3-CPMe$_3$ ligand forms an essentially symmetric cap over the triangular metal face. Bond distances and angles about each metal atom are sufficiently similar so that the Fe and Co atoms are indistinguishable. Selected bond distances and angles of **3a** are listed in Table IX.

The C–PR$_3$ group on metal complexes can be described as a (trialkylphosphino)methylidyne ligand,[23] and it has now been structurally characterized in terminally bonded[23] as well as doubly[25] and triply bridging[8,26] modes. The (trimethylphosphino)methylidyne ligand of **3a** features a short C–PMe$_3$ bond (1.715 (3) Å) in comparison to the three equivalent P–CH$_3$ distances (1.792 (3) Å). This bond length is comparable to C–PMe$_3$ distances found in related compounds: $[W_2(CPMe_3)_2(PMe_3)_4Cl_4][AlCl_4]_2$ (1.71 (3) Å),[23] $Zr_2[(CH_2)_2PMe_2]_4(\mu\text{-}CPMe_3)_2$ (1.688 (4) Å),[25] and $(Ph_3PAu)_3CPMe_3$ (1.62 (4) and 1.83 (3) Å for two independent molecules in the unit cell).[26] In comparison to organic ylides, the C=P distance is 1.661 (8) Å in $H_2C{=}PPh_3$[27] and 1.648 (7) Å in O=C=C=PPh$_3$.[28]

(25) Rice, G. W.; Ansell, G. B.; Modrick, M. A.; Zentz, S. *Organometallics* **1983**, *2*, 154.

(26) Schmidbaur, H.; Scherbaum, F.; Huber, B.; Müller, G. *Angew. Chem., Int. Ed. Engl.* **1988**, *27*, 419.

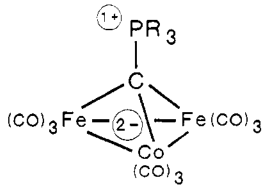

Figure 5. Charge-separated formulation of a $[Fe_2Co(CO)_9(CPR_3)]^-$ cluster.

Trends and Comparisons of $[Fe_2Co(CO)_8(PR_3)(CCO)]^-$ and $[Fe_2Co(CO)_9(CPR_3)]^-$ Clusters. Figure 4 illustrates the relationship between ν_{CO} and ligand basicity for both series of phosphine-substituted clusters **2a–f** and **3a–e**. The value of ν_{CO} is obtained from the most intense band in the infrared spectrum of each compound while ligand basicity is represented by ΔHNP, which is the difference between half neutralization potentials of the free phosphine ligand and *N,N′*-diphenylguanidine in nitromethane.[29,30] Since phosphine substitution for CO results in an increase in the electron density at the metal framework, the expected trend of decreasing ν_{CO} with increasing ligand basicity is observed for each series of substituted clusters. It is noteworthy that the clusters with PR$_3$ coordinated to the carbon atom have ν_{CO} values that are 9–16 cm^{-1} lower than the corresponding clusters with PR$_3$ bonded to the Co metal center. The phosphine ligand is therefore a more effective electron donor from the capping carbon atom than from the Co metal center, which is consistent with the formulation of these compounds as organometallic ylides. A charge-separated representation of **3a–e** places a formal 2– charge at the cluster core and a formal 1+ charge on the phosphorus atom (Figure 5).

Carbon–carbon and carbon–phosphorus coupling constants for the C–CO and C–PR$_3$ ligands unfortunately give no insight into the bonding nature of the capping group. The values of $^1J_{CC}$ (**2a–f**) and $^1J_{PC}$ (**3a–e**) do not appear to correlate with either the basicity or size of the phosphine ligand. However, it can at least be noted that $^1J_{CC}$ for **2a–e** is smaller than the 79.4 Hz coupling observed for **1**,[3] which suggests that CO substitution of **1** by phosphines results in a decreased C–C bond order for the ketenylidene ligand.

Reaction times for forming **2a–f** and **3a–e** were qualitatively observed during the generation of each compound in CH$_2$Cl$_2$ solution. The reactions were typically run at ambient temperature by using 1.2–10 M excesses of phosphine or phosphite and monitored either by IR or ^{1}H NMR spectroscopy. The qualitative rates vary significantly depending on the nature of the ligand. Substitution to form **2a–f** from **1** ranges from <30 min for PMe$_3$ (1.2 equiv) to over a day for P(OPh)$_3$ (10 equiv). However, there is no apparent correlation with ligand nucleophilicities. For instance, P(OMe)$_3$ and PEt$_3$ substitute for CO on **1** in roughly the same amount of time under the same conditions. Reaction times for the complete transformation of **1** to **3a–e** vary from about 30 min for PMe$_3$ to several days for P(OMe)$_3$. No migration of P(OPh)$_3$ from the Co to carbon atom was observed for **2f** after 2 weeks at room temperature. The ease with which the ylide-capped clusters **3a–e** form appear to be qualitatively related to the relative nucleophilicities of the phosphine

(27) Bart, J. C. J. *J. Chem. Soc. B* **1969**, 350.

(28) Daly, J. J.; Wheatly, P. J. *J. Chem. Soc. A* **1966**, 1703.

(29) Streuli, C. A. *Anal. Chem.* **1960**, *32*, 985.

(30) ΔHNP values (mV): PMe$_3$, 114; PMe$_2$Ph, 281; PMePh$_2$, 424; PEt$_3$, 111; P(OMe)$_3$, 580; P(OPh)$_3$, 875. The value for P(OMe)$_3$ in an estimate. Values taken from: (a) Thorsteinson, E. M.; Basolo, F. *J. Am. Chem. Soc.* **1966**, *88*, 3929. (b) Chang, C.-Y.; Johnson, C. E.; Richmond, T. G.; Chen, Y.-T.; Trogler, W. C.; Basolo, F. *Inorg. Chem.* **1981**, *20*, 3167.

Table X. ^{13}C NMR Data for Mixed-Metal Fe-Co Clusters[a]

compound	temp, °C	^{13}C NMR,[b] ppm
$HFe_2Co(CO)_9(CPMe_3)$ (4)	−90	213.4, 210.7, 210.0, 206.8, 203.8 (2:2:1:2:2, CO), 202.1 (d, $^1J_{PC}$ = 30.4 Hz, μ_3-C)
$Fe_2Co_2(C)(CO)_{11}(PMe_3)$ (5)[c]	−60[d]	474.0 (μ_4-C), 214.7 (3, a, $Fe(CO)_3$), 212.0 (3, b, $Fe(CO)_3$), 202.8 (1, c, $Co(CO)_2(PMe_3)$), 202.2 (3, d, $Co(CO)_3$), 200.5 (1, c, $Co(CO)_2(PMe_3)$)
	−120[d]	475.2 (μ_4-C), 218.3 (1, a), 216.8 (1, a), 214.0 (1, b), 213.6 (1, b), 211.1 (1, a), 210.7 (1, b), 203.5 (1, c), 202.2 (3, d), 200.4 (1, c)
[PPN][$Fe_2Co(CO)_7$(dmpm)(CCO)] (6)	−90	225.5 (1, $Fe(CO)_2P$), 219.6 (3, $Fe(CO)_3$), 218.9 (1, $Fe(CO)_2P$), 214.7 (1, $Co(CO)_2P$), 206.8 (1, $Co(CO)_2P$), 191.3 (ds, $^1J_{CC}$ = 58.6 Hz, CCO), 103.9 (br, CCO)[e]
$Fe_2Co(CO)_8$(dmpm)(CH) (7)	−70	270.5 (d, $^1J_{CH}$ = 161.3 Hz, μ_3-CH), 258.6 (1, d, J_{PC} = 14.2 Hz, μ-CO), 216.8 (1, d, J_{PC} = 11.0 Hz, $Fe(CO)_2P$), 213.3 (3, $Fe(CO)_3$), 206.0 (1, $Co(CO)_2$ P), 204.6 (1, d, J_{PC} = 22.0 Hz, $Fe(CO)_2P$), 203.9 (1, $Co(CO)_2P$)
$Fe_2Co(CO)_8$(dmpm)(CMe) (8)	−90	302.2 (μ_3-CMe), 259.5 (1, μ-CO), 216.3 (1, d, J_{PC} = 15.2 Hz, $Fe(CO)_2P$), 211.6 (3, Fe-$(CO)_3$), 206.5 (1, $Co(CO)_2P$), 204.8 and 204.5 (2, overlapping signals of $Fe(CO)_2P$ and $Co(CO)_2P$)
$Fe_2Co(CO)_7$(dmpm)(CCOMe) (9)	−60	219.1 (1, d, J_{PC} = 14.8 Hz, $Fe(CO)_2P$), 217.1 (1, d, J_{PC} = 8.6 Hz, $Fe(CO)_2P$), 216.1 (3, $Fe(CO)_3$), 214.7 (1, $Co(CO)_2P$), 205.1 (1, $Co(CO)_2P$), 160.4 (ds, $^1J_{CC}$ = 43.5 Hz, CCOMe), 156.6 (br, CCOMe)[e]

[a] CD_2Cl_2 solution unless noted otherwise. All resonances are singlets unless noted: d, doublet; ds, doublet on singlet. [b] Integers in parentheses are integrated intensities. [c] Refer to text and Figure 6 for references to the lettering scheme. [d] 1:2 $CD_2Cl_2/CHFCl_2$ solution. [e] Assignment confirmed by selective ^{13}C enrichment.[3]

ligands. The time for complete reaction roughly increases in the order of $PMe_3 < PEt_3$, $PMe_2Ph < PMePh_2 < P(OMe)_3$.

The reactions of 1 with phosphine ligands represent the first instances of a formal nucleophilic attack at the capping carbon atom of a ketenylidene ligand. In previous cluster chemistry, nucleophilic attack occurs exclusively at the carbonyl carbon atom of the CCO ligand by the addition of a negatively charged substrate.[1-3] Phosphine attack on the ketenylidene ligand of [$WCl_2(CO)(PMePh_2)_2$(CCO)] has been proposed, but this mononuclear CCO-containing complex has not been directly observed.[31] Despite the ease with which most [$Fe_2Co(CO)_9(CPR_3)$]$^-$ clusters are formed, phosphine displacement of CO from the carbon vertex of $M_3(CO)_9$(CCO) clusters is not a general reaction. The $P(OPh)_3$ ligand of **2f** shows no propensity to migrate and cationic [$Co_3(CO)_8(PPh_3)$(CCO)]$^+$ is also stable with respect to phosphine migration.[20] Thus the relative affinities of carbonyl and phosphine ligands for carbon and metal centers appear to be delicately balanced in these clusters.

Although phosphine substitution at the carbon atom of a metal cluster has not been observed previously, an analogous reaction is known for the boron atom of a μ_3-BCO ligand.[32] In that instance, the conversion of $H_3Os_3(CO)_9$(BCO) to $H_3Os_3(CO)_9(BPMe_3)$ occurs by direct substitution at the capping boron atom.[33] Phosphine addition reactions to unsaturated carbon sites of multinuclear metal complexes is well-known.[17,34,35] Such reactions provide a more common route to cluster-bound ylides. Intramolecular phosphine migration is relatively rare but has been observed in a few other cases. Phosphine mobility over the face of a Pt_3 cluster is known[36] and the

Scheme II

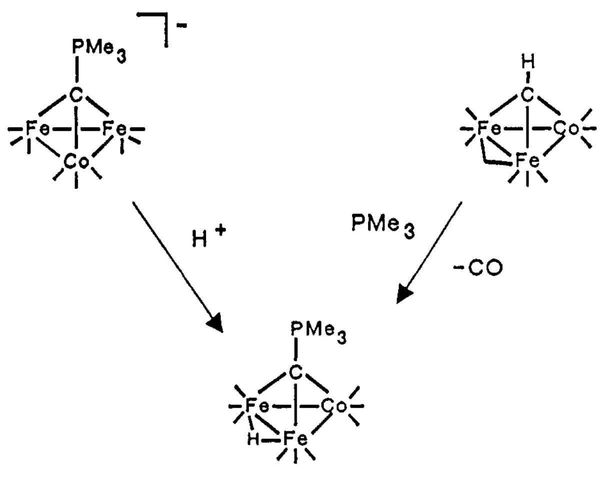

4

migration of phosphine ligands from the vinylidene group to a Co center has been reported for another mixed-metal Fe–Co cluster.[17]

An analogy can be drawn between CO substitution of [$Fe_2Co(CO)_9$(CCO)]$^-$ (1) and ligand substitution of tetrametal carbonyl clusters. From theoretical bonding models, compound 1 can be viewed as a tetrahedral cluster based on a heteroatomic Fe_2CoC core surrounded by 10 carbonyl ligands.[37-39] Thus the conversion of μ_3-CCO to μ_3-CPR_3 is analogous to ligand substitution on a $M(CO)_3$ vertex.

Reactivity of [PPN][$Fe_2Co(CO)_9(CPMe_3)$] (3a). Under an atmosphere of CO, **3a** cannot be reconverted to 1. However, free ^{13}CO does undergo exchange with the CO ligands on the cluster. No further reaction occurs between **3a** and excess PMe_3 or with other phosphine ligands such as PEt_3 and $P(OMe)_3$. In contrast to the facile CO substitution reactions with phosphines, [$Fe_2Co(CO)_9$(CCO)]$^-$ does not react with stoichiometric amounts of NMe_3 and a large excess (>100 equiv) of amine leads to slow decomposition of the cluster. Thus the analogous cluster-bound nitrogen ylide was not synthesized.

Unlike 1, which undergoes protonation to cleave the CCO ligand and forms a methylidyne species,[3] **3a** is pro-

(31) List, A. K.; Hillhouse, G. L.; Rheingold, A. L. *J. Am. Chem. Soc.* **1988**, *110*, 4855.
(32) Shore, S. G.; Jan, D.-Y.; Hsu, L.-Y.; Hsu, W.-L. *J. Am. Chem. Soc.* **1983**, *105*, 5923.
(33) Shore, S. G., private communication.
(34) (a) Churchill, M. R.; DeBoer, B. G.; Shapley, J. R.; Keister, J. B. *J. Am. Chem. Soc.* **1976**, *98* 2357. (b) Henrick, K.; McPartlin, M.; Deeming, A. J.; Hasso, S.; Manning, P. *J. Chem. Soc., Dalton Trans.* **1982**, 899. (c) Deeming, A. J.; Manning, P. *J. Organomet. Chem.* **1984**, *265*, 87. (d) Adams, R. D.; Babin, J. E.; Tsai, M. *Organometallics* **1987**, *6*, 1717.
(35) (a) Wong, Y. S.; Paik, H. N.; Chieh, P. C.; Carty, A. J. *J. Chem. Soc., Chem. Commun.* **1975**, 309. (b) Carty, A. J.; Mott, G. N.; Taylor, N. J.; Ferguson, G.; Khan, M. A.; Roberts, P. J. *J. Organomet. Chem.* **1978**, *149*, 345. (c) Belmonte, P.[Schrock, R. R.; Churchill, M. R.; Youngs, W. J. *J. Am. Chem. Soc.* **1980**, *102*, 2858. (d) Uedelhoven, W.; Neugebauer, D.; Kreissl, F. R. *J. Organomet. Chem.* **1981**, *217*, 183. (e) Jeffery, J. C.; Navarro, R.; Razay, H.; Stone, F. G. A. *J. Chem. Soc., Dalton Trans.* **1981**, 2471.
(36) Bradford, A. M.; Jennings, M. C.; Puddephatt, R. J. *Organometallics* **1988**, *7*, 792.
(37) Wade, K. *Adv. Inorg. Chem. Radiochem.* **1976**, *18*, 1.
(38) Mingos, D. M. P. *Acc. Chem. Res.* **1984**, *17*, 311.
(39) Hoffmann, R. *Angew. Chem., Int. Ed. Engl.* **1982**, *21*, 711.

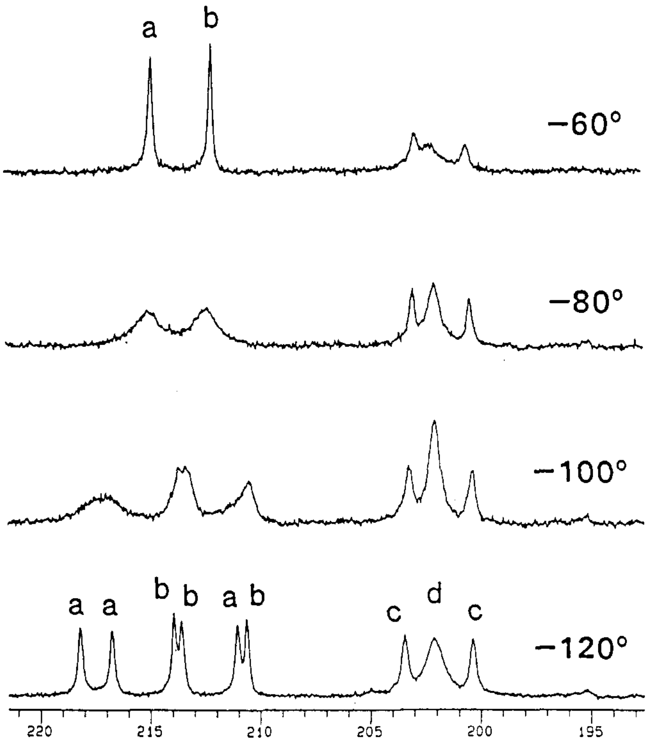

Figure 6. Variable-temperature ^{13}C NMR spectra (100.577 MHz) of the carbonyl region of $Fe_2Co_2(C)(CO)_{11}(PMe_3)$ (**5**) recorded in 1:2 $CD_2Cl_2/CHFCl_2$.

tonated on the metal framework, yielding $HFe_2Co(CO)_9(CPMe_3)$ (**4**) (Scheme II). The ^{13}C NMR spectrum of **4** (Table X) indicates that the cluster has C_s symmetry, which requires the hydride to be in a bridging position across the Fe–Fe bond or a triply bridging site. Compound **4** can also be generated by treatment of $Fe_2Co(CO)_{10}(CH)$ with PMe_3, a reaction in which the phosphine induces C–H bond cleavage (Scheme II). When this reaction was monitored by ^1H, ^{31}P, and ^{13}C NMR spectroscopies at low temperature, complicated spectra were obtained that suggested the presence of numerous intermediates. However, **4** is produced cleanly upon completion of the reaction.

The C–PMe_3 bond of **3a** can be cleaved in a cluster-building reaction with $Co_2(CO)_8$ (eq 2) which generates a butterfly carbide cluster, $Fe_2Co_2(C)(CO)_{11}(PMe_3)$ (**5**), and

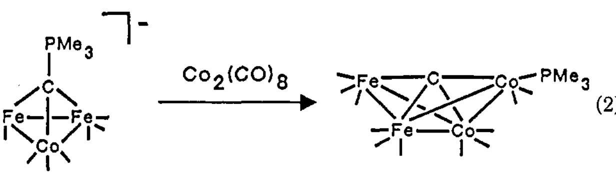

(2)

5

+ $[Co(CO)_4]^-$

+ 2CO

a substantial amount of $Co_4(CO)_{12}$. The ^{13}C NMR spectrum of **5** exhibits a characteristic carbide resonance at 475.2 ppm.[40] Resonances in the carbonyl region are assigned on the basis of chemical shifts, peak broadness, and variable-temperature behavior (Table X). However, even though resonances of $Fe(CO)_3$, $Co(CO)_3$, and $Co(CO)_2(PMe_3)$ vertices are clearly identified, the positions of these vertices within the butterfly framework cannot be determined conclusively. (The positions shown in eq 2 are

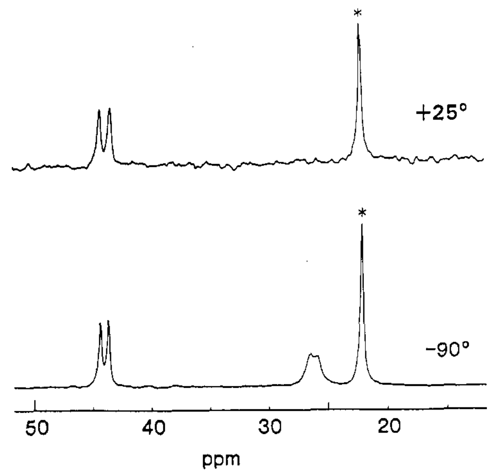

Figure 7. Variable-temperature ^{31}P NMR spectra (109.16 MHz) of $[PPN][Fe_2Co(CO)_7(dmpm)(CCO)]$ (**6**) recorded in CD_2Cl_2. The peak marked with an asterisk is due to PPN^+.

assigned arbitrarily.) Variable-temperature ^{13}C NMR spectra of **5** are shown in Figure 6. The molecule has C_1 symmetry and consequently resonances from carbonyl ligands of four distinct metal vertices are observed (a–d). As the temperature is raised from −120 to −60 °C, the deshielded resonances due to the two $Fe(CO)_3$ vertices (a and b) coalesce and then sharpen, while the broad and more shielded resonances due to the $Co(CO)_3$ and $Co(CO)_2(PMe_3)$ vertices (c and d) become even broader.

Synthesis and Characterization of $[PPN][Fe_2Co(CO)_7(dmpm)(CCO)]$ (6). Attempts to crystallize $[Fe_2Co(CO)_8(PR_3)(CCO)]^-$ compounds (**2a–f**) were unsuccessful despite numerous tries. Even **2f**, which is stable with respect to phosphine migration, was only obtained as an oil. A synthesis was therefore devised for a related, but more easily crystallized cluster. Treatment of **1** with dmpm (dmpm = bis(dimethylphosphino)methane) results in displacement of two CO ligands and the formation of $[PPN][Fe_2Co(CO)_7(dmpm)(CCO)]$ (**6**) (eq 3). The bite

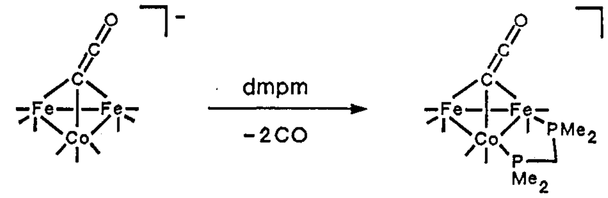

(3)

6

of dmpm is sufficiently small so that the chelating ligand is confined to coordinate at the metal framework. Use of a diphosphine ligand with a larger bite results in chelation between metal and carbon atoms.[41]

Compound **6** crystallizes readily and was spectroscopically characterized prior to a single-crystal X-ray diffraction study. The IR spectrum of **6** displays a strong band at 1939 cm^{-1}, which is 25 cm^{-1} lower than the strong band observed for the analogous PMe_3-substituted cluster **2a**. Addition of an extra phosphine group thus significantly enhances electron density on the metal framework. At −90 °C two ^{31}P NMR signals are observed in a slightly second-order pattern, and 77-Hz coupling is clearly distinguishable on both resonances (Figure 7). The broader, more shielded resonance becomes unobservably broad at +25 °C while the more deshielded resonance remains

(40) Bradley, J. S. *Adv. Organomet. Chem.* **1983**, *22*, 1.

(41) Ching, S.; Jensen, M. P.; Sabat, M.; Shriver, D. F., *Organometallics*, following paper in this issue.

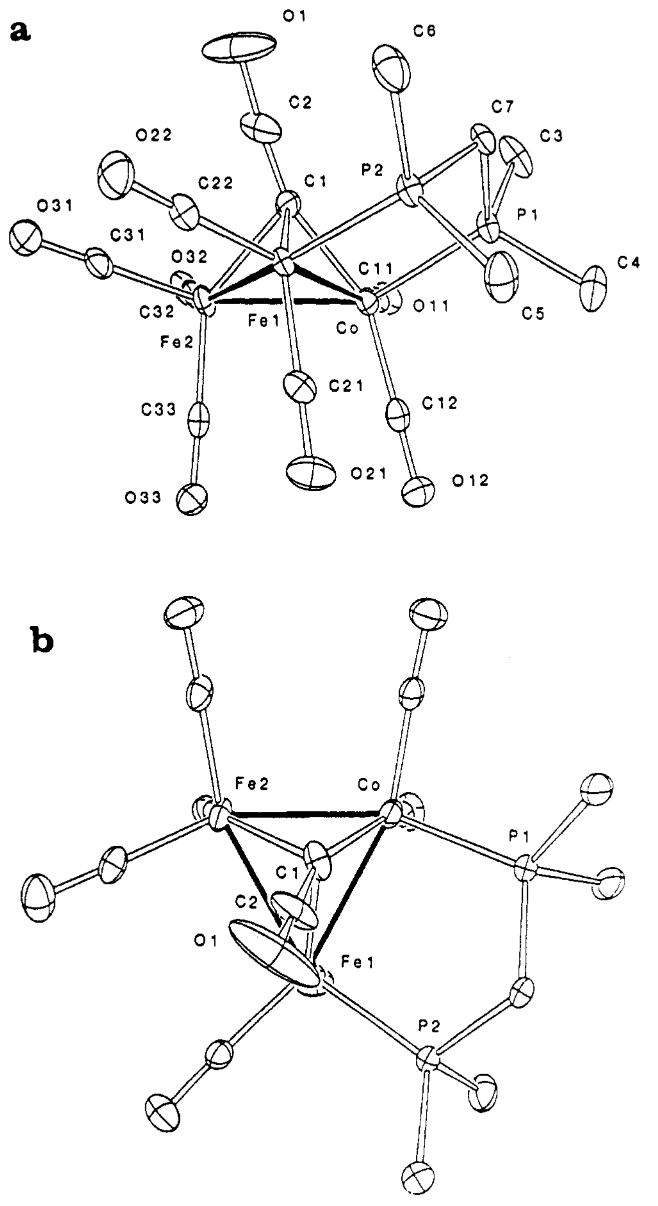

Figure 8. a. An ORTEP drawing of the cluster anion in $[PPN][Fe_2Co(CO)_7(dmpm)(CCO)]·CH_2Cl_2$ ($6·CH_2Cl_2$). The atoms are represented by 30% probability thermal ellipsoids. b. An alternate view of $[Fe_2Co(CO)_7(dmpm)(CCO)]^-$ from the CCO-capped side of the cluster.

relatively sharp. This behavior is consistent with dmpm chelation across an Fe–Co bond, with line broadening of one resonance being due to phosphine coordination to the quadrupolar Co atom. The ^{13}C NMR data for **6** (Table X) further support dmpm chelation across a Fe–Co bond. Of the resonances due to metal-bound carbonyl ligands, the signals at 214.7 and 206.8 ppm broaden considerably with increasing temperature. These resonances are assigned to Co-bound carbonyl ligands, with the more deshielded resonance being attributed to an axially bonded CO.[15] Similar assignments apply for the Fe-bound carbonyl resonances at 225.5 and 218.9 ppm. The ketenylidene ligand exhibits resonances at 191.3 and 103.9 ppm with C–C coupling of 58.6 Hz, which is significantly lower than the $^1J_{CC}$ values observed for **1** and **2a–f**.

A single crystal of $[PPN][Fe_2Co(CO)_7(dmpm)(CCO)]·CH_2Cl_2$ (**6**·CH_2Cl_2) suitable for an X-ray structure determination was grown by slow diffusion of Et_2O into a 1:1 CH_2Cl_2/Et_2O solution containing the cluster. The molecular structure of the cluster anion is shown in parts a and b of Figure 8. The dmpm ligand occupies equatorial positions on adjacent metal atoms, and the chelated metal–metal distance is elongated by 0.03 Å relative to the other two metal–metal bonds. It was not possible to crystallographically distinguish Co and Fe atoms in the structure of **6**, so Co and Fe1 are assigned arbitrarily. The C1—C2 (1.221 (6) Å) and C2–O1 (1.181 (6) Å) distances of the ketenylidene ligand are within error of the analogous distances found in **1** (C–C, 1.29 (5) Å; C–O, 1.20 (4) Å),[3] but the C1—C2 distance is short compared to ketenylidene C=C bond lengths that have been precisely determined.[7,42,43] The CCO ligand in **6** tilts toward one of the phosphine-substituted metal centers and is slightly offset over a metal–metal bond (Figure 8b). The least-squares line through the CCO forms a 37° angle with the line perpendicular to the plane of metal atoms. Tilted ketenylidene ligands are not unusual and have been similarly observed in $[Ph_4As]_2[Fe_3(CO)_9(CCO)]$ (33°),[4] $[PPN][Fe_2Co(CO)_9(CCO)]$ (30°),[3] and $[Ph_4P]_2[Os_3(CO)_9(CCO)]$ (26°).[7] However, ketenylidene ligands typically tilt directly over a metal atom, whereas the CCO ligand in **6** tilts slightly over a metal–metal bond. This difference may be a result of steric interactions with the dmpm ligand. Nonbonded distances from C2 to Fe1 and Fe2 are 2.424 (5) and 2.749 (5) Å, respectively. Selected bond distances and angles of **6** are listed in Table XI.

Table XI. Selected Bond Distances (Å) and Angles (deg) for $[PPN][Fe_2Co(CO)_7(dmpm)(CCO)]•CH_2Cl_2$ (6•CH_2Cl_2)

Bond Distances			
Co–Fe1	2.569 (1)	Fe2–C2	2.749 (5)
Co–Fe2	2.537 (1)	C1–C2	1.221 (6)
Fe1–Fe2	2.535 (1)	C2–O1	1.181 (6)
Co–C1	1.894 (4)	P1–C3	1.829 (5)
Fe1–C1	1.994 (4)	P1–C4	1.797 (5)
Fe2–C1	1.953 (4)	P1–C7	1.828 (4)
Co–P1	2.183 (1)	P2–C5	1.816 (5)
Fe1–P2	2.187 (1)	P2–C6	1.818 (5)
Fe1–C2	2.424 (5)	P2–C7	1.830 (4)
Bond Angles			
Co–Fe1–Fe2	59.61 (2)	C11–Co–C12	99.0 (2)
Fe1–Fe2–Co	60.86 (2)	C11–Co–P1	96.9 (1)
Fe1–Co–Fe2	59.53 (2)	C12–Co–C1	146.0 (2)
Co–C1–Fe1	82.7 (2)	C12–Co–P1	102.7 (1)
Co–C1–Fe2	82.5 (2)	P1–Co–Fe1	95.89 (4)
Fe1–C1–Fe2	79.9 (1)	C21–Fe1–C22	103.0 (2)
Co–C1–C2	158.5 (4)	C21–Fe1–C1	134.4 (2)
Fe1–C1–C2	94.8 (3)	C21–Fe1–P2	97.7 (1)
Fe2–C1–C2	118.2 (4)	C22–Fe1–P2	99.8 (1)
C1–C2–O1	171.9 (5)	P2–Fe1–Co	94.86 (3)
Co–P1–C7	112.8 (1)	C31–Fe2–C32	99.4 (2)
Fe1–P2–C7	110.8 (1)	C31–Fe2–C33	102.0 (2)
C3–P1–C4	100.9 (2)	C32–Fe2–C33	101.9 (2)
C5–P2–C6	102.6 (2)	C33–Fe2–C1	135.1 (2)
P1–C7–P2	109.9 (2)		

The CCO tilt in **6** can be viewed as a semibridging interaction between the carbon-bound carbonyl group and one of the phosphine-coordinated metal centers. Phosphine substitution for CO is known to induce carbonyl bridging in other clusters.[44,45] In an anionic, electron-rich cluster such as **6**, a semibridging CO may serve to alleviate the buildup of electron density on the metal framework. An increase in the CCO tilt may also facilitate phosphine

(42) Crespi, A. M.; Went, M. J.; Sunshine, S. S.; Shriver, D. F. *Organometallics* **1988**, *7*, 214.
(43) Sailor, M. J.; Shriver, D. F. *Organometallics* **1985**, *4*, 1476.
(44) (a) Malatesta, L.; Caglio, G. *Chem. Commun.* **1967**, 420. (b) Albano, V.; Bellon, P.; Scatturin, V. *Chem. Commun.* **1967**, 730. (c) Karel, J. J.; Norton, J. R. *J. Am. Chem. Soc.* **1974**, *96*, 6812.
(45) (a) Matheson, T. W.; Robinson, B. H.; Tham, W. S. *J. Chem. Soc. A* **1971**, 1457. (b) Penfold, B. R.; Robinson, B. H. *Acc. Chem. Res.* **1973**, *6*, 73.

Scheme III

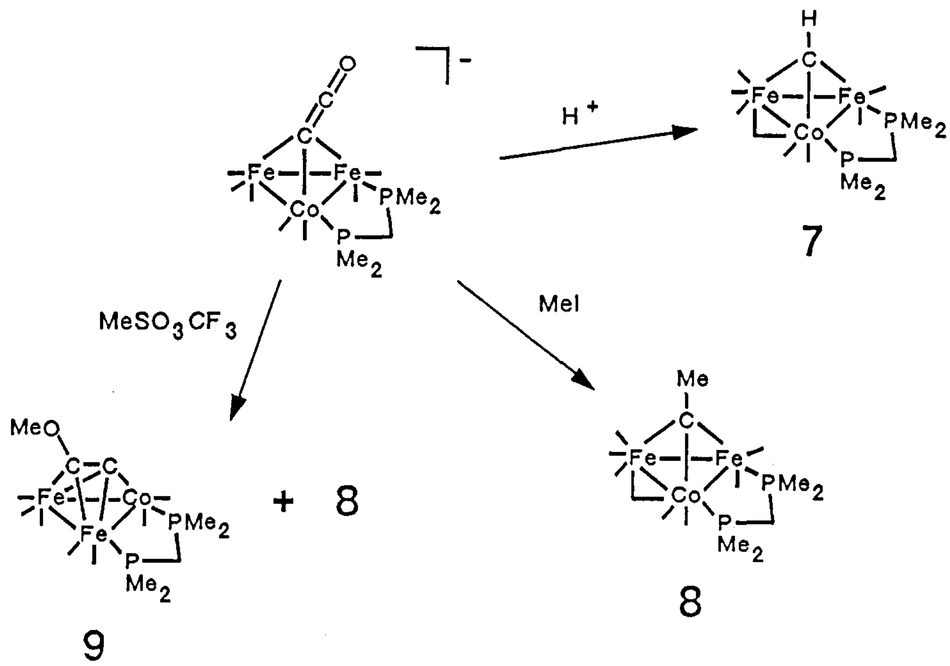

migration in clusters such as **2a–e** since the ketenylidene CO is drawn closer to the metal framework. Such speculation, however, is based on the assumption that the structure of **6** is maintained to some extent in solution. There is yet no conclusive evidence that either supports or disproves a tilted ketenylidene ligand in solution. Calculations indicate that the precession of a tilted CCO about the face of a trimetallic cluster is a facile process with a barrier of ca. 3 kcal/mol.[7,20] Thus the tilting phenomenon has not been observed by NMR spectroscopy, while Raman experiments have proven to be insensitive to this structural detail.[46] Crystal packing forces can also be invoked to explain the CCO tilt in **6** although there are no obvious steric interactions between the cluster and the PPN cation or CH_2Cl_2 molecule of crystallization.

Reactivity of [PPN][$Fe_2Co(CO)_7$(dmpm)(CCO)] (6). The presence of dmpm in **6** results in CO ligands that are more labile toward exchange and a CCO ligand that is more susceptible to electrophilic attack compared to **1**.[3] Under 1 atm of ^{13}CO at room temperature, **6** undergoes ^{13}CO enrichment at all eight CO groups to give [$Fe_2Co(^*CO)_7$(dmpm)(C*CO)]$^-$. Carbonyl exchange reaches equilibrium within 24 h, which is much more rapid than the 4 days required for CO exchange with **1**.[3] Treatment of **6** with HSO_3CF_3 leads to immediate protonation of the capping carbon atom to give a methylidyne-capped cluster, $Fe_2Co(CO)_8$(dmpm)(CH) (**7**) (Scheme III), which is analogous to the protonation of **1**. Interestingly, **1** does not react with cationic methylating reagents, but **6** reacts with CH_3I to give $Fe_2Co(CO)_8$(dmpm)(CMe) (**8**) and with $CH_3SO_3CF_3$ to give a 1:2 mixture of **8** and the acetylide-containing species $Fe_2Co(CO)_7$(dmpm)(CCOMe) (**9**) (Scheme III). This pattern of reactivity is more akin to the dinegatively charged cluster [$Fe_3(CO)_9(CCO)$]$^{2-}$ than **1**.[4,5]

Compounds **7–9** have been isolated and spectroscopically characterized. Analogous structures are proposed for **7** and **8**, each with a capping alkylidyne ligand and a bridging CO across the non-dmpm-bridged Fe–Co bond. The ^{13}C NMR spectrum of **7** recorded at −70 °C exhibits deshielded resonances at 270.5 and 258.6 ppm that are characteristic of μ_3-CH and μ-CO ligands in this type of cluster[3,4] (Table X). The terminal CO region contains a peak at 213.3 ppm due to the $Fe(CO)_3$ vertex and two pairs of peaks due to carbonyl ligands of the phosphine-substituted metal centers. The peak at 206.0 and 203.9 ppm broaden with increasing temperature and are thus assigned to Co-bound carbonyl ligands. The small chemical shift difference between these two resonances relative to that in **6** suggests that axial and equatorial carbonyl bonding has been distorted at the Co atom, and this in turn favors the placement of the bridging CO at this site. The remaining doublets at 216.8 and 204.6 ppm are respectively assigned to axial and equatorial carbonyl ligands on the dmpm-coordinated Fe atom. Similar spectroscopy is observed for **8**. The acetylide ligand in **9** is easily identified by comparing its ^{13}C NMR signals with those of similar acetylide-containing clusters.[5] Carbonyl ligands on Fe and Co atoms in **9** are assigned analogously to those in **7** and **8** by using line broadening as an indication of Co-bound CO ligands (Table X). The orientation of the acetylide ligand is believed to be the one shown in Scheme III, with the Co–C–C plane bisecting the Fe–Fe bond. This is supported by the small chemical shift difference between the peaks at 219.1 and 217.1 ppm due to carbonyl ligands of the chelated Fe vertex, which indicates that axial and equatorial CO bonding has been perturbed at this site. By contrast, resonances of the CO ligands on the Co atom are separated by almost 10 ppm, so normal axial–equatorial bonding is believed to be maintained. A crystal structure of [PPN][$Fe_3(CO)_9(CCOC(O)CH_3)$] shows that the two Fe atoms that are bisected by the acetylide ligand have CO ligands that are disrupted from regular axial and equatorial bonding.[5]

Conclusions

The interaction of [$Fe_2Co(CO)_9(CCO)$]$^-$ has been studied with numerous phosphine ligands. For simple phosphines a general, two-step process is observed in which initial substitution at the Co metal center is followed by phosphine migration to the capping carbon atom. The resulting [$Fe_2Co(CO)_9(CPR_3)$]$^-$ clusters can be considered organometallic ylides, and this formulation is supported by in-

(46) Sailor, M. J.; Went, M. J.; Shriver, D. F. *Inorg. Chem.* 1988, *27*, 2666.

frared data. The CO substitution reaction cannot be extended to bulky phosphines, and the rate of the migration step is qualitatively related to phosphine basicity.

The effects of phosphine substitution on the structure and reactivity of the CCO ligand were examined in the case of $[Fe_2Co(CO)_7(dmpm)(CCO)]^-$. This cluster contains a ketenylidene ligand that is tilted toward one of the phosphine-substituted metal centers. The chemistry of $[Fe_2Co(CO)_7(dmpm)(CCO)]^-$, in comparison to $[Fe_2Co(CO)_9(CCO)]^-$, indicates that the dmpm ligand labilizes the CO ligands toward exchange with gaseous ^{13}CO and increases the susceptibility of the CCO ligand toward electrophilic attack.

Phosphine migrations have recently become more prevalent in organometallic chemistry, and fluxional[36] and irreversible[8,17] processes are now known. But despite the ease with which $[Fe_2Co(CO)_9(CPR_3)]^-$ clusters are generated, ligand migration does not occur in all phosphine-substituted ketenylidene clusters as noted by the stability of $[Co_3(CO)_8(PPh_3)(CCO)]^+$.[20] Thus the relative affinities of carbonyl and phosphine ligands for a capping carbon atom appear to be delicately balanced. The propensity for phosphines to undergo migration in the $[Fe_2Co(CO)_8(PR_3)(CCO)]^-$ clusters may be related to the unique ability of anionic ketenylidene clusters to exchange the CO group of the CCO ligand with free CO.[3-6] This in turn may be related to the charge on the cluster.

Acknowledgment. This research was supported by the NSF Synthetic Inorganic and Organometallic Chemistry Program.

Registry No. 1, 88657-64-1; **2a**, 119145-53-8; **2b**, 119145-55-0; **2c**, 119145-57-2; **2d**, 119145-59-4; **2e**, 119145-61-8; **2f**, 119145-63-0; **3a**, 109284-18-6; **3b**, 119145-65-2; **3c**, 119145-67-4; **3d**, 119145-69-6; **3e**, 119145-71-0; 4, 109284-19-7; **5**, 119145-72-1; **6**, 119145-74-3; **6**·CH_2Cl_2, 119239-74-6; **7**, 119145-75-4; **8**, 119145-76-5; **9**, 119145-77-6; dmpm, 64065-08-3; ^{59}Co, 7440-48-4; PMe_3, 594-09-2; PMe_2Ph, 672-66-2; $PMePh_2$, 1486-28-8; PEt_3, 554-70-1; $P(OMe)_3$, 121-45-9; PPh_3, 603-35-0; PCy_3, 2622-14-2; HSO_3CF_3, 1493-13-6; $Co_2(CO)_8$, 10210-68-1; $Co_4(CO)_{12}$, 17786-31-1.

Supplementary Material Available: Tables of anisotropic thermal parameters, positional parameters not listed in the text, and bond distances and angles not listed in the text, and a packing diagram of the unit cell of $[PPN][Fe_2Co(CO)_7(dmpm)(CCO)]\cdot CH_2Cl_2$ (10 pages); a listing of observed and calculated structure factors (37 pages). Ordering information is given on any current masthead page.

A Diphosphine Ligand as a Bridge between Carbide and Metal Centers in Clusters

Stanton Ching, Michael P. Jensen, Michal Sabat, and Duward F. Shriver*

Department of Chemistry, Northwestern University, Evanston, Illinois 60208

Received September 14, 1988

The reaction of $[PPN][Fe_2Co(CO)_9(CCO)]$ with dmpe (dmpe = 1,2-bis(dimethylphosphino)ethane) generates an ylide-capped cluster, $[PPN][Fe_2Co(C)(dmpe)(CO)_8]$ (1), in which dmpe bridges the carbide ligand and cobalt atom. Protonation of 1 occurs across the Fe–Fe bond to give $HFe_2Co(C)(dmpe)(CO)_8$ (2), which retains the ylide moiety but has the phosphine bonded to an Fe center on the metal framework instead of the Co atom. Treatment of 1 with $Co_2(CO)_8$ leads to the isolation of $FeCo_2(CO)_9(\mu_3\text{-}CPMe_2CH_2CH_2Me_2PFe(CO)_4)$ (3), in which dmpe bridges between the cluster and a mononuclear species. Clusters 1–3 are all spectroscopically characterized. The molecular structure of 3 has been determined by single-crystal X-ray diffraction. Compound 3 crystallizes in the space group $P1$ with $a = 9.392$ (1) Å, $b = 10.847$ (2) Å, $c = 7.946$ (1) Å, $\alpha = 107.76$ (1)°, $\beta = 110.56$ (1)°, $\gamma = 88.73$ (1)°, $V = 718.5$ (4) Å^3, and $Z = 1$.

Introduction

Our current research on the reactivity of $[Fe_2Co(CO)_9(CCO)]^-$ with phosphine ligands was prompted by the discovery of an unusual substitution–isomerization sequence which ultimately generates a capping ylide moiety from a capping ketenylidene ligand.[1,2] In the course of these studies we have synthesized a new ylide-containing cluster, $[Fe_2Co(C)(dmpe)(CO)_8]^-$ (dmpe = 1,2-bis(dimethylphosphino)ethane), in which the diphosphine ligand chelates across a metal–carbon bond. We thought that this type of chelation might stabilize the ylide moiety in cluster-building reactions. We discovered previously that the reaction of $[Fe_2Co(CO)_9(CPMe_3)]^-$ with $Co_2(CO)_8$ results in degradation of the ylide group and produces a carbide-containing cluster, $Fe_2Co_2(C)(CO)_{11}(PMe_3)$, along with significant quantities of $Co_4(CO)_{12}$.[2] In this paper, we report the synthesis of $[PPN][Fe_2Co(C)(dmpe)(CO)_8]$ and its reactivity with acid and $Co_2(CO)_8$.

Experimental Section

General Procedures and Materials. All manipulations were performed under a purified N_2 atmosphere by using standard Schlenk and syringe techniques[3] or in a Vacuum Atmospheres drybox unless noted otherwise. Solvents were distilled from appropriate drying agents and deaerated with N_2 before use.[4] Dmpe (Strem) was used as received (dmpe = 1,2-bis(dimethylphosphino)ethane). HSO_3CF_3 (Aldrich) was distilled before use.

(1) Ching, S.; Sabat, M.; Shriver, D. F. *J. Am. Chem. Soc.* 1987, *109*, 4722.
(2) Ching, S.; Sabat, M.; Shriver, D. F., *Organometallics*, preceding paper in this issue.
(3) Shriver, D. F.; Drezdzon, M. A. *The Manipulation of Air-Sensitive Compounds*, 2nd ed.; Wiley: New York, 1986.
(4) Gordon, A. J.; Ford, R. A. *The Chemist's Companion*; Wiley: New York, 1972.

